AN ABSTRACT OF THE THESIS OF

SCOTT ALEXANDER CHAMBERS for the degree of DOCTOR OF PHILOSOPHY

in Chemistry presented on July 7, 1977

Title: SATELLITE STRUCTURE IN THE GAS-PHASE X-RAY PHOTOELECTRON SPECTRA OF PLANAR UNSATURATED MOLECULES

Abstract approved: Redacted for privacy

T. Darrah Thomas

The satellite structure ("shake-up") present in the X-ray photoelectron spectra of several planar molecules containing double bonds has been investigated in the gas phase. This set consists of three five-membered heterocyclic molecules, ethylene and two of its fluorinated analogs, and benzene with three of its fluorinated analogs. In addition, core ionization potentials have been accurately measured for the heterocyclic molecules.

It is found that measuring satellites in the gas phase provides a clearer picture than do previous measurements done in the solid phase for the heterocyclic molecules; inelastic scattering structure, which is present in the same energy region as shake-up satellites can be easily minimized in the gas phase but not in the solid phase.

Theoretical predictions of the relative intensities and energies of the satellites have been made within the

sudden approximation using CNDO/2 wave functions. Agreement between theory and experiment is fair (within about a factor of two), suggesting that such wave functions are only of qualitative value. The distinct low-energy satellites present in the spectra have been assigned to transitions from occupied to unoccupied π orbitals. The unresolved high-energy satellites are, however, not so clearly understood. According to the theory, they are due in part to one-electron excitations in the valence σ orbitals. However, certain high-energy satellites presumably result from single excitations to Rydberg-like or continuum orbitals ("shake-off") and multiple excitations. States such as these are not predicted by the theory because of the limited basis set.

The wave functions are used to study charge rearrangement accompanying core ionization. It is found that in general, electrons are transferred from the atoms possessing the most electron density in the ground ionic state as the excited ionic states are populated. In certain cases, there is a direct relationship between the atomic character of the molecular orbitals involved in a given shake-up transition and the transition energies for core ionization at the different atoms. In many cases, the low-lying excited states of the ion are essentially those of the neutral molecule. However, if the molecular symmetry is modified by photoionization, other charge rearrangements that would not be expected from consideration of the neutral species can take place.

Satellite Structure in the Gas-Phase X-Ray Photoelectron Spectra of Planar Unsaturated Molecules

by

Scott Alexander Chambers

A THESIS

submitted to

Oregon State University

in partial fulfillment of
the requirements for the
degree of

Doctor of Philosophy

Completed July 7, 1977

Commencement June 1978

APPROVED:

Redacted for privacy

Professor of Chemistry
in charge of major

Redacted for privacy

Chairman of the Department of Chemistry

Redacted for privacy

Dean of Graduate School

Date thesis is presented July 7, 1977

Typed by Deanna L. Cramer for Scott Alexander Chambers

ACKNOWLEDGEMENTS

I am indebted to Professor T. Darrah Thomas, who has been instrumental in this phase of my scientific development. His ability to cut to the heart of a problem and proceed to solve it served as a very useful guide for me in learning to do the same more effectively. I have appreciated the financial support provided by the National Science Foundation, the U.S. Energy Research and Development Administration, and the Oregon State University Department of Chemistry.

I am grateful to Professor Victor Madsen and Dr. Carl Kocher of the OSU Department of Physics for many stimulating discussions during the course of the research.

Special thanks are extended to Dr. James Jen and Dr. Steve Smith for their willingness to help me learn to operate the spectrometer with all its idiosyncrasies.

I have benefited from the insight of other members of our research group: Drs. Robert Shaw, Thomas Carroll, Seppo and Helena Aksela, Mr. Pat Sitton and Mr. Ken Bomben. Special thanks are due to Mr. Ken Bomben, whose unique sense of humor managed to produce something to laugh about at the most exasperating moments during life in this laboratory.

Mr. John Archibald has been very helpful in machining various parts for the spectrometer and Mr. Doyle Woodrow has maintained numerous electronic devices used during operation

of the spectrometer; I thank them both for their service.

Finally, and with deepest gratitude, I wish to thank my wife, Judy, whose love, support, and interest in this project provided much encouragement during these years of graduate study, and to my parents, who supported my efforts completely.

TABLE OF CONTENTS

Table of Contents -- continued

LIST OF TABLES

LIST OF FIGURES

SATELLITE STRUCTURE IN THE GAS-PHASE X-RAY PHOTOELECTRON SPECTRA OF PLANAR UNSATURATED MOLECULES

I. GENERAL INTRODUCTION

During the last ten years, X-ray photoelectron spectroscopy has emerged as a powerful and versatile tool for studying a wide variety of phenomena of physical and chemical interest. Its scope includes gas, liquid, and solid phases. At first, attention was given almost exclusively to the "primary" photolines in the spectra. These result from the photoejection of a core electron, leaving behind an ion with one electronic vacancy but no other excitation of the molecule. In this case, the conservation of energy equation for the photoelectric effect assumes the form,

$$h\nu = E_i + K \quad , \tag{1.1}$$

where E_i, the ionization potential, is the difference between initial and final state energies, $h\nu$ is the photon energy and K is the kinetic energy of the ejected electron. In the simplest theoretical treatment, E_i is equated to an orbital energy from a self-consistent field calculation (1) (Koopmans' theorem).

However, even in the earliest experiments (2), satellite bands were observed on the low kinetic energy side of the primary peak. The intensities observed ranged from

approximately 2 to 20% of that of the primary peak. The process that gives rise to satellites was regarded as simultaneous K-shell ionization and valence shell excitation. It was rationalized that the perturbation brought about by ejection of a core electron causes promotion of a valence electron to an unoccupied or continuum state. Thus the phrases "shake-up" and "shake-off" were adopted as appropriate titles for these two descriptions of the observed phenomenon.

Well above threshold, the K-shell electron is ejected with high energy, resulting in a minimum of interaction with the ion. This feature has made possible application of the sudden approximation (3) to satellite prediction. Several workers have utilized the sudden approximation, using wave functions of varying sophistication, to predict energies and intensities of observed satellites in noble gases (2), small molecules (4), inorganic solids (5), and polymers (6). These experiments allow one to test rather critically the quality of wave functions, in that detailed agreement between theory and experiment requires wave functions of high accuracy. Once the quality of a wave function has been determined by this means, it can be used to deduce information on charge distribution in the initial and final states and to assign orbital transitions to the satellites. It has been shown that the smallest systems of interest such as Ne (7) and HF (8) require very sophisticated wave

functions to provide accurate descriptions of their electronic structure, whereas, at least for qualitative purposes, larger molecules such as substituted benzenes (9) and organic polymers (6) are adequately described by intermediate-level molecular orbitals.

Studying satellite structure in the gas phase is preferable to that in the solid phase because in the latter, high background and energy-loss structure are unavoidable. Energy-loss results from inelastic collisions as the photoelectrons leave the solid. However, in the absence of special high temperature ovens, one is somewhat limited in what one can study in the gas phase. Nevertheless, for purposes of understanding the essential phenomena that give rise to satellites, small molecules are desirable because of the ease of getting them into the gas phase and the relative simplicity of performing theoretical calculations for them. Thus, it has been the purpose of this work to measure in the gas phase and theoretically calculate the satellite structure of several heterocyclic and fluorinated hydrocarbons. Included in this set are furan, pyrrole, thiophen, benzene and three of its fluorinated analogs, and ethylene with two of its fluorinated analogs. The heterocyclics were chosen specifically so that the gas-phase results could be compared with previous measurements done in the solid phase (10) and to test, by comparison with theory, previous interpretations of the data. The fluorinated

hydrocarbons were chosen to see how the degree of fluorination affects the satellite structure. Clark (11,12) has found that in the case of pyridine, perfluoropyridine, cyclohexene and perfluorocyclohexene, the carbon 1s satellites resulting from $\pi \rightarrow \pi^*$ transitions are somewhat more intense in the fluorinated molecules than in their non-fluorinated analogs.

For theoretical insight, CNDO/2 (complete neglect of differential overlap) approximate molecular orbital wave functions (13) have been used to predict the observed experimental spectra. Agreement is fair (within about a factor of two), suggesting that such wave functions are only of qualitative value. The theory has been used to differentiate between transitions involving σ and π molecular orbitals in these planar molecules and to derive information about the charge rearrangement accompanying core photoionization.

II. THEORY OF SATELLITES

The Photoelectric Cross Section

It is well known (14) that absorption of infrared radiation by a molecule leads to the population of a multiplicity of rotational states as vibrational excitation occurs. Similarly, a manifold of vibrational states are populated within the electronic state excited by absorption of visible or ultraviolet light (15). So it is reasonable to expect that absorption of a photon of sufficient energy to excite an electron into the continuum will populate a manifold of electronic states of the ion. Indeed, Condon (16) predicted satellite structure in photoelectron spectra long before it was observed. It is essentially the dipole interaction of the radiation with the molecule that gives rise to these spectroscopic effects.

Martin and Shirley (17) have developed the theory of satellite structure accompanying core ionization in some detail. They derive a general expression for the photoelectric cross section in the dipole approximation using single determinantal wave functions. This treatment is fairly rigorous and when extended to include configuration interaction for both initial and final states, leads to excellent quantitative agreement with experiment for Ne (7) and HF (8). In order to illustrate the interesting physics

of the process, the following simplified discussion is presented.

The general expression for the photoelectric cross section of an N-electron system interacting with the dipole component of a radiation field (18) is

$$\sigma(\omega) = C(\omega)\left|\langle\Psi_f(N)\left|\hat{e}\cdot\sum_{\ell=1}^{N}\vec{P}_\ell\right|\Psi_i(N)\rangle\right|^2\rho(E_f) \quad . \qquad (2.1)$$

Here $C(\omega)$ is inversely proportional to the photon energy, $\hat{e}$ is the radiation polarization vector, $\vec{P}_\ell$ is the momentum operator for the ℓth electron, and $\rho(E_f)$ is the density of states for the emitted photoelectrons. The operator carries the system from some initial state $\Psi_i(N)$ to a final state $\Psi_f(N)$ that is composed of a free electron eigenstate and a wave function for the ion.

If the photon energy is substantially greater than the binding energy of the core electrons, the above expression can be simplified greatly. First, all ejected electrons will have high kinetic energies as dictated by the conservation of energy equation (Eq. 1.1). The implications of high-energy ejected electrons are important to a simple theoretical development. The classical notion of a fast moving particle quantum mechanically corresponds to an outgoing electron that will not interact with the ion strongly enough to cause excitation. Thus, a high-energy outgoing electron may be described approximately by a single continuum wave

function χ. Ignoring antisymmeterization for the moment, the eigenstates may be factored into products of active and passive orbitals

$$\Psi_i(N) = \phi_1(1)\Psi_{KT}(N-1) \tag{2.2a}$$

$$\Psi_f(N) = \chi\ \Psi'_o(N-1)\ . \tag{2.2b}$$

Here, ϕ_1 is the active orbital from which the electron is to be ejected, $\Psi_{KT}(N-1)$ is the Koopmans'-theorem state for the system with a K-shell vacancy, and $\Psi'_o(N-1)$ is the eigenstate for the ion with a core vacancy in its ground electronic state.

The second simplification that results from large photon energies relative to the highest binding energies is that all one-electron transition moments for other than the K-shell electrons are negligible; the X-ray absorption cross section falls off rapidly as the difference between photon energy and binding energy becomes large. As a result, the sum in Eq. 2.1 reduces to one term of two factors and gives what is essentially the partial cross section for the ground state of the ion,

$$\sigma_o(\omega) = C(\omega)\left|\langle\chi|\hat{e}\cdot\vec{P}_1|\phi_1(1)\rangle\ \langle\Psi'_o(N-1)|\Psi_{KT}(N-1)\rangle\right|^2\rho(E_f)\,. \tag{2.3}$$

If one assumes that the passive orbitals remain "frozen" in the ion, then $\Psi'_o(N-1)$ is identical to $\Psi_{KT}(N-1)$,

suggesting that only the ground state of the ion is populated. In this case, the cross section is proportional to the transition moment for the core electron, with no dependence on the states of any of the other electrons. Thus the spectrum contains only one peak, in conflict with the experimental observation of satellites accompanying the primary peak. The passive electrons do not remain frozen, but relax toward the site of core ionization. The effective nuclear charge of the core ionized atom is increased by order e relative to the neutral atom and the remaining charge flows toward the hole in the ground state of the ion. As a result, Ψ_o' is not identical to Ψ_{KT}. The two functions are eigenstates of different Hamiltonians and the square of their overlap is less than unity. The overlap of certain other electronically excited states containing the same core vacancy with Ψ_{KT} comprises the rest of the final-state intensity. Therefore, all electronically excited ionic configurations formed by single and multiple valence electron excitations from the ground ionic state into both unoccupied and continuum orbitals must be added to the ground ionic state for a complete description of all final states of the ion. Thus, the extent of electronic relaxation in the sample determines the distribution of intensity over various final states of the ion -- extensive relaxation resulting in substantial satellite intensity.

A case in point is nickel carbonyl (see Appendix A). Hillier and Saunders have shown that an ab initio better-than-minimal basis set calculation predicts lower core ionization potentials (resulting from more extra-atomic relaxation toward the core hole) in the carbon and oxygen K-shell spectra of $Ni(CO)_4$ than those of the carbon monoxide molecule (19). Although quantitative agreement is lacking, the same trend has been observed in our gas-phase studies (20) as well as those of Barber and co-workers done in the solid phase (21). On the basis of the evident increase in extra-atomic relaxation, one would expect much more intense satellites in the carbon and oxygen 1s spectra of $Ni(CO)_4$ than in those of CO. This is in fact observed in both the solid (22) and gas phases (20).

In order for a particular final state Ψ_j' to have a non-zero overlap with Ψ_{KT}, it must be of the same spatial and spin symmetry as Ψ_{KT}. Therefore, a monopole selection rule ($\Delta J = \Delta L = \Delta S = \Delta M_J = \Delta M_S = 0$) governs the intensities of final states. Inserting an expansion over all possible final states into the expression for the cross section for the ground ionic state leads to the total photoelectric cross section,

$$\sigma(\omega) = C(\omega)\left|\langle\chi|\hat{e}\cdot\vec{P}_1|\phi_1(1)\rangle\right|^2 \sum_j \left|\langle\Psi_j'(N-1)|\Psi_{KT}(N-1)\rangle\right|^2 \rho(E_f). \tag{2.4}$$

Thus, the total photoelectric cross section is a sum of partial cross sections, each giving the probability of a

different final state of the ion. As Fadley has shown in a similar derivation (23), $\sigma(\omega)$ contains information about all one-electron and multielectron transitions.

Relative intensities may be obtained by taking ratios of partial cross sections. For photon energies far from threshold, $\langle\chi|\hat{e}\cdot\vec{P}_1|\phi_1(1)\rangle$ varies slowly over the energy range containing the various final ionic state energies, and to first approximation cancels in calculating partial cross section ratios. Thus for a particular excited final ionic state j, the intensity relative to that of the ground state is,

$$P'_j = \frac{|\langle\Psi'_j|\Psi_{KT}\rangle|^2}{|\langle\Psi'_o|\Psi_{KT}\rangle|^2} \quad . \tag{2.5}$$

It is interesting to note that the above expression is also obtainable by the sudden approximation. This equivalence results from the assumption made that the ejected electron is of sufficient energy that its interaction with the ion is negligible -- an assumption also made in applying the sudden approximation to the photoemission process. As Martin and Shirley have more rigorously shown (17), the sudden approximation is indeed the high photoelectron energy limit of the dipole approximation.

Although Eq. 2.5 has been derived for simple product wave functions, it can also be derived for Slater determinants (17). The wave functions chosen may be inserted into

this expression and the resulting intensities compared with experimental results, providing a highly sensitive reflection of the accuracy of the wave functions.

The Quality of Wave Functions

The extent to which a wave function can reproduce experimental satellite intensities is a sensitive test of its accuracy. The results of such tests shed light on the degree of theoretical sophistication necessary to describe a particular kind of system. Because of the nature of the molecular electronic Hamiltonian, highly accurate solution of the Schrödinger equation requires a basis of determinantal wave functions, each describing a particular electron configuration. In accord with the variational principle, a sufficiently complete linear expansion in this basis is necessary for a quantitatively accurate wave function. Such techniques of configuration interaction bridge the gap between the Hartree-Fock limit and what is at least in principle an exact solution. In regard to satellite intensity prediction, it has been shown (7,8) that such "superposition of configuration" wave functions are essential to a complete description of the initial and final states. Also, in cases where the photoelectron is not of sufficient energy to justify use of the sudden approximation, a single continuum eigenstate no longer adequately describes the photoelectron, and interchannel coupling must be included (24). In this case, the

final-state wave function is a configuration expansion that couples terms containing continuum and ionic eigenstates to the proper symmetry to obey the overall dipole selection rule. The monopole selection rule for the formation of excited ionic states no longer has any meaning because the dipole cross section does not factor into active and passive electron functions.

These calculations are quite involved and require vast amounts of computer time. Although the quantitative agreement that results is quite satisfying and of great theoretical value, such accuracy is not often required for the purposes of many experimentalists. Many times an approximate technique is far more attractive because of its tractability, low expense, and retention of basic physical concepts such as molecular orbitals and electron spin. When configuration interaction is introduced, the concept of an orbital no longer has any meaning and electron spin is much more difficult to keep track of. However, the question arises, what levels of approximation are necessary to qualitatively describe various kinds of molecules? One might expect that if a bonding system is sufficiently delocalized, a minimal or valence basis set and single determinants from a self-consistent field calculation would suffice. Testing the validity of this hypothesis has been one of the goals of the present work. The SCF method used here has been the complete neglect of differential overlap approximation to

the Hartree-Fock method introduced by Pople, Santry, and Segal (13) (hereafter referred to as CNDO/2 or CNDO).

The CNDO Approximation

The essence of the CNDO method is to assume that all products of atomic orbitals for a given electron are negligible unless the orbitals are the same. (The atomic basis set consists of Slater orbitals.) For example, if ϕ_μ and ϕ_ν represent two atomic orbitals of different atoms, the product $\phi_\mu(1)\phi_\nu(1)$ is neglected in normalizing the molecular orbitals and in calculating many of the Hamiltonian matrix elements if μ is not the same as ν. However, if μ is the same as ν, the product is retained. When this assumption is applied to the evaluation of two-electron repulsion integrals, a substantial reduction of labor results. The non-zero repulsion integrals are further reduced to one value per atom pair, resulting in the following simplification,

$$\iint \phi_\mu^*(1)\phi_\nu^*(1)\frac{1}{r_{12}}\phi_\lambda(2)\phi_\sigma(2)d\tilde{\tau}_1 d\tilde{\tau}_2 \equiv (\mu\nu|\lambda\sigma)$$

$$= \delta_{\mu\nu}\delta_{\lambda\sigma}(\mu\mu|\lambda\lambda) \equiv \gamma_{AB} \cdot \begin{matrix}\phi_\mu \text{ on atom A} \\ \mu_\lambda \text{ on atom B}\end{matrix} \qquad (2.6)$$

The inner electrons (n=1 for first row elements and n=1 and 2 for second row elements) are not treated explicitly, but rather as part of an inert core along with the nucleus. Thus, the core Hamiltonian is of the form

$$H = -\frac{1}{2}\nabla^2 + \sum_B V_B \ , \qquad (2.8)$$

where V_B is the potential due to the nucleus and core electrons of atom B. The core Hamiltonian matrix elements are obtained semiempirically; a complete discussion of the parametrization may be found in the original reference (13).

In its original form, the CNDO/2 method (13) is parametrized for hydrogen through fluorine and sodium through chlorine. However, it is straightforward to obtain by quadratic extrapolation using the method of second differences, empirical parameters for neon and argon that are consistent with those for the other first and second row atoms. These parameters are listed in Table 1; the fluorine parameters are in good agreement with those obtained by Clark and Adams (12).

Table 1. Empirical parameters used in CNDO/2 calculations involving neon and argon (eV).

	Neon	Argon
$-\beta_A^\circ$	49	47.951
$\frac{1}{2}(I_s + A_s)$	39.962	25.856
$\frac{1}{2}(I_p + A_p)$	13.182	10.621
$\frac{1}{2}(I_d + A_d)$		1.311
G^{1a}	0.640257	
F^{2a}	0.367210	

[a]Used in the INDO calculation.

The calculation for a neutral molecule is done in the usual way. For an ion, the equivalent-cores model (25) is used. In this method, the assumption is made that core ionization of an atom is equivalent to the addition of a proton to the nucleus. Thus a K-shell vacancy of a certain atom is represented by the atom with the next higher Z value. Because the Franck-Condon principle is assumed to hold for photoemission well above threshold, the ground state molecular geometry is used in doing the equivalent-cores calculation for the various ions. After one has calculated orbitals for the molecule and various states of the ion, Slater determinants are readily constructed and scalar products may be calculated to give probabilities for the creation of various shake-up states. The scalar product of two determinantal wave functions is itself a determinant composed of overlaps of the spin-orbitals from the two determinantal wave functions. Thus, the problem of calculating satellite probabilities at the SCF level of approximation is one of evaluating a determinant composed of overlap integrals between orbitals from the molecular determinant and those from the various ionic-state determinants. In the SCF approximation, the one-electron orbital overlaps are of the form

$$\langle \Psi_i | \Psi'_j \rangle = \sum_{\mu} \sum_{\nu} C_{i\mu} C'_{j\nu} \langle \phi_\mu | \phi_\nu \rangle \ . \qquad (2.9)$$

Under the assumption of CNDO, this simply reduces to

$$\langle \Psi_i | \Psi'_j \rangle = \sum_{\mu} \sum_{\nu} C_{i\mu} C'_{j\nu} \delta_{\mu\nu} = \sum_{\mu} C_{i\mu} C'_{j\mu} \ , \qquad (2.10)$$

In certain cases, the results of the full determinantal calculation are very similar to those obtained by taking the overlap of active one-electron orbitals -- one from the molecule and one from the ion. The determinant that leads to the probability of shake-up from orbital N in the molecule to orbital N'+1 in the equivalent-cores ion is of the form

$$\langle f|i \rangle = \begin{vmatrix} \langle 1'|1\rangle & \langle 1'|2\rangle & \langle 1'|3\rangle & \cdots & \langle 1'|N\rangle \\ \langle 2'|1\rangle & \langle 2'|2\rangle & \langle 2'|3\rangle & \cdots & \langle 2'|N\rangle \\ \vdots & & & & \\ \langle N'-1|1\rangle & \langle N'-1|2\rangle & \langle N'-1|3\rangle & \cdots & \langle N'-1|N\rangle \\ \langle N'+1|1\rangle & \langle N'+1|2\rangle & \langle N'+1|3\rangle & \cdots & \langle N'+1|N\rangle \end{vmatrix} . \qquad (2.11)$$

If there is near orthonormality between molecular and ionic orbitals, the off-diagonal matrix elements would be very small and all diagonal elements except $\langle N'+1|N\rangle$ would be nearly unity. Thus, the value of the determinant would be nearly equal to the one-electron orbital overlap $\langle N'+1|N\rangle$. Several workers have used this overlap to calculate shake-up probabilities without considering any other matrix elements (4,9). However, if near orthonormality between molecular and ionic orbitals does not exist, the value of the determinant is no longer well approximated by $\langle N'+1|N\rangle$. For

several of the calculations done in this work, a discrepancy of as much as a factor of two exists in the two methods of calculation mentioned above. Therefore, all reported shake-up probabilities are results of the full determinantal calculation.

The Role of Electron Spin

One of the most frequently populated shake-up states results from single valence electron excitation simultaneous with core ionization. Such a state possesses three unpaired electrons -- one in the core and two in the valence shell. Therefore, a proper treatment of the role of electron spin in shake-up necessitates considering the coupling of three spin $\frac{1}{2}$ particles. As is well known, three spin $\frac{1}{2}$ particles couple to two doublets and a quartet. Because of the monopole selection rule derived earlier, there is no intensity to the quartet state.

In the molecules studied here, there is extensive delocalization among the valence electrons. Therefore it is safe to assume that the exchange interaction between the two unpaired valence electrons in the shake-up state will be much larger than that between the valence electrons and the core electron. In this case, the valence electrons couple to a singlet and a triplet, which in turn couple to the core electron to yield two doublets and a quartet. By solving the three-electron coupling problem in detail, Carroll and

Thomas (26) have shown that under the assumption of negligible exchange interaction between the core and unpaired valence electrons, only the doublet corresponding to a singlet valence configuration is appreciably populated. One key result of their derivation is that the shake-up probability for excitation from valence orbital B in the molecule to unoccupied orbital C' in the ion equals $2|\langle C'|B\rangle|^2$. The factor of two arises because of the presence of two electrons originally in orbital B.

In the limit of absolutely no interaction between the valence electrons and the core, the problem simplifies considerably and yet yields the same result as that which Carroll and Thomas derived. The simplifying feature is that the wave function for the core electron may be separated from the wave function for the valence electrons, leaving only a two-particle coupling problem to be solved. Consider the Koopmans-theorem state of the molecule to have two valence electrons in orbital B. Furthermore, let the shake-up state differ from the ground ionic state by a single excitation from orbital B' to orbital C'. The monopole selection rule forbids population of the valence triplet state in the limit of no interaction with the core. Therefore, the determinantal wave functions for the Koopmans'-theorem state, the ground ionic state, and shake-up state may be written as

$$\Psi_{KT} = \frac{1}{\sqrt{2}} [BB(\alpha\beta - \beta\alpha)] \qquad (2.12)$$

$$\Psi'_o = \frac{1}{\sqrt{2}} [B'B'(\alpha\beta - \beta\alpha)] \qquad (2.13)$$

$$\Psi'_1 = \frac{1}{\sqrt{2}} [(B'C' + C'B')(\alpha\beta - \beta\alpha)] \; . \qquad (2.14)$$

The probability of the ground ionic state is given by

$$|\langle\Psi'_o|\Psi_{KT}\rangle|^2 = S^2_{BB'} \; , \qquad (2.15)$$

where $S_{BB'} = \langle B|B'\rangle$. Similarly, the probability of the shake-up state is

$$|\langle\Psi'_1|\Psi_{KT}\rangle|^2 = 2S^2_{BB'}S^2_{BC'} \; . \qquad (2.16)$$

If there is near orthonormality between the molecular orbitals B and C and the ionic orbitals B' and C', $S_{BB'}$ may be approximately equated to 1 to give for the intensity of the shake-up state, $2S^2_{BC'}$. This result is identical to that of Carrol and Thomas. As mentioned earlier, the breakdown in the assumption of near orthonormality between the molecular and ionic orbitals often necessitates replacing $S_{BC'}$ with an overlap of Slater determinants.

In summary, for molecules with delocalized valence electrons, only shake-up states with valence singlet configurations will be appreciably populated. This conclusion

was reached by Basch in his calculations of the satellite structure in formaldehyde (27).

Vibrational Broadening in Satellites

A commonly observed feature in core photoelectron spectra is increased line widths of the satellites relative to the primary peak. The broadening of satellites can originate from two sources -- overlapping electronic states and the population of more vibrational levels than would occur in a ground ionic state. The former occurs especially when, as in the case of several of the molecules studied here, chemically inequivalent atoms are present. In this case, shake-up as well as ground states with core vacancies on the different atoms may lie so close in energy as to be experimentally unresolvable. Vibrational broadening in primary core photoelectron peaks was not taken seriously until recently. Prior to the publication of a convincing argument by Gelius (28), it was believed that because K-shell electrons are nonbonding, their excitation into the continuum would not alter the vibrational population in the final state. As Gelius has demonstrated, the presence of a core vacancy substantially alters the charge distribution, resulting in different equilibrium bond distances in the final state. Therefore, several vibrational states could be populated in the ground electronic state of the ion.

Now consider a shake-up state. Here not only has a core electron been ejected but also a nonbonding or bonding valence electron has been promoted to an anti-bonding orbital. One would expect that the equilibrium bond distances would be greatly perturbed by such a transition, resulting in even more vibrational broadening than what is present in the ground ionic state. Such "vibrational shake-up" is predicted in exactly the same way as is electronic shake-up in the sudden approximation. As Gelius has shown (28), inclusion of the eigenstates for nuclear motion along with the electronic wave functions, together with the Born-Oppenheimer approximation leads, to a product of probabilities for electronic and vibrational shake-up. The latter are the Franck-Condon factors for the various transitions.

The Correction to Orbital Energies of Virtual States

Within the orbital approximation, a shake-up state is described as one in which the valence shell possesses different orbital occupancy than the ground state of the ion, both having the same core vacancy. The energy difference between the ground state and shake-up state is rigorously the difference in their total energies. If the valence shell rearrangement in the shake-up state consists of the promotion of a single electron, one might expect that the energy difference would approximately reduce to the difference in orbital energies for the two orbitals involved

in the transition. In this model, relaxation of the passive electrons toward the new vacancy in the valence shell is completely neglected, resulting in energies expected to be slightly in excess of the true energies. However, this approach leads to energies that are frequently a factor of two larger than experimental results, making it impossible to account for the error on the basis of neglect of relaxation alone. The dilemma is inherent in the SCF method.

The orbital energies calculated from the Hartree-Fock method are eigenvalues of a Hamiltonian based on a ground-state orbital occupancy. To calculate the energy of an unoccupied orbital, one places a hypothetical electron in that orbital and calculates its interaction with all the other particles, represented by the following diagram:

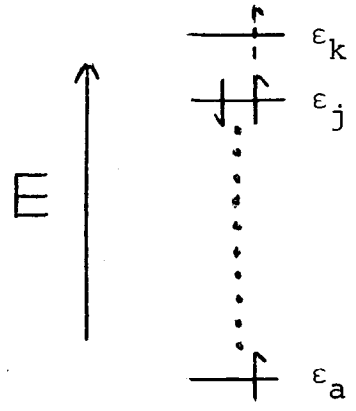

However, if one neglects exchange interaction of the core and valence electrons, the actual electron configuration of the shake-up state we are considering can be represented by a second diagram:

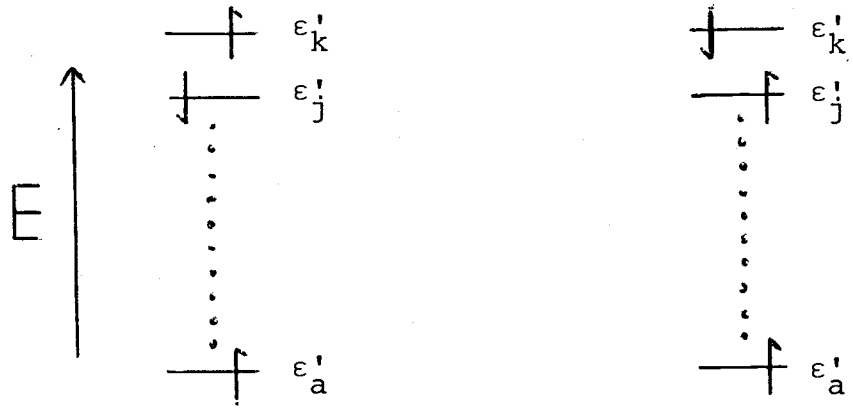

The wave function for the shake-up state is actually a linear combination of these two configurations. If one compares the two diagrams, it is evident that the orbital energy difference $\varepsilon_k - \varepsilon_j$ from the ground state configuration will be in excess of the true shake-up energy because the expression for ε_k essentially contains interactions of an electron in the kth molecular orbital with itself in the jth molecular orbital. Therefore, in order to use orbital energies from an equivalent-cores model calculation (represented by the first diagram) to predict shake-up energies, these interactions must be removed. Relaxation toward the valence hole is still neglected in this treatment, leading one to expect calculated energies that are too large, but not by a factor of two.

Roothaan (29) has derived this result from considerations of the correct wave functions for a closed shell system and various excited state configurations. Assuming no degeneracy in either state and no spin-orbit coupling, he shows that for a single excitation from a closed shell

$$\Delta E = \varepsilon_k - \varepsilon_j - (J_{kj} - K_{kj} \pm K_{kj}) \quad . \qquad (2.17)$$

where the plus sign holds for the triplet final state and the minus sign holds for singlet final state.

The above equation, using CNDO/2 orbital energies, was utilized to calculate shake-up energies for the singlet valence configurations resulting from one-particle promotions of all valence electrons into all unoccupied orbitals of the ion.

III. EXPERIMENTAL MEASUREMENTS OF SATELLITES

Origin and Purity of Samples

All samples investigated in this study are gases or liquids at room temperature; the liquids have sufficient vapor pressure for gas-phase measurements. The various suppliers (Aldrich, Malinckrodt, and PCR) indicated a minimum purity of 97% for each compound, although specific purity analysis by the suppliers revealed 99.5% purity or higher for many of the samples. No further purification was attempted.

Procedures for Taking X-ray Photoelectron Spectra

All measurements reported here were accomplished on our cylindrical electrostatic analyzer (30) using either $AlK\alpha_{1,2}$ or $MgK\alpha_{1,2}$ x-radiation. Both of these characteristic X-rays are spin-orbit split doublets. However, the $MgK\alpha_{1,2}$ X-ray has a slightly smaller full width at half maximum than does the corresponding aluminum X-ray (31). Therefore, magnesium was used in experiments where higher resolution than what is possible with aluminum was needed.

The X-ray tube used in this study, designed by S. R. Smith (32), is the second generation to be developed for our analyzer. In its most recent stage, the tube is

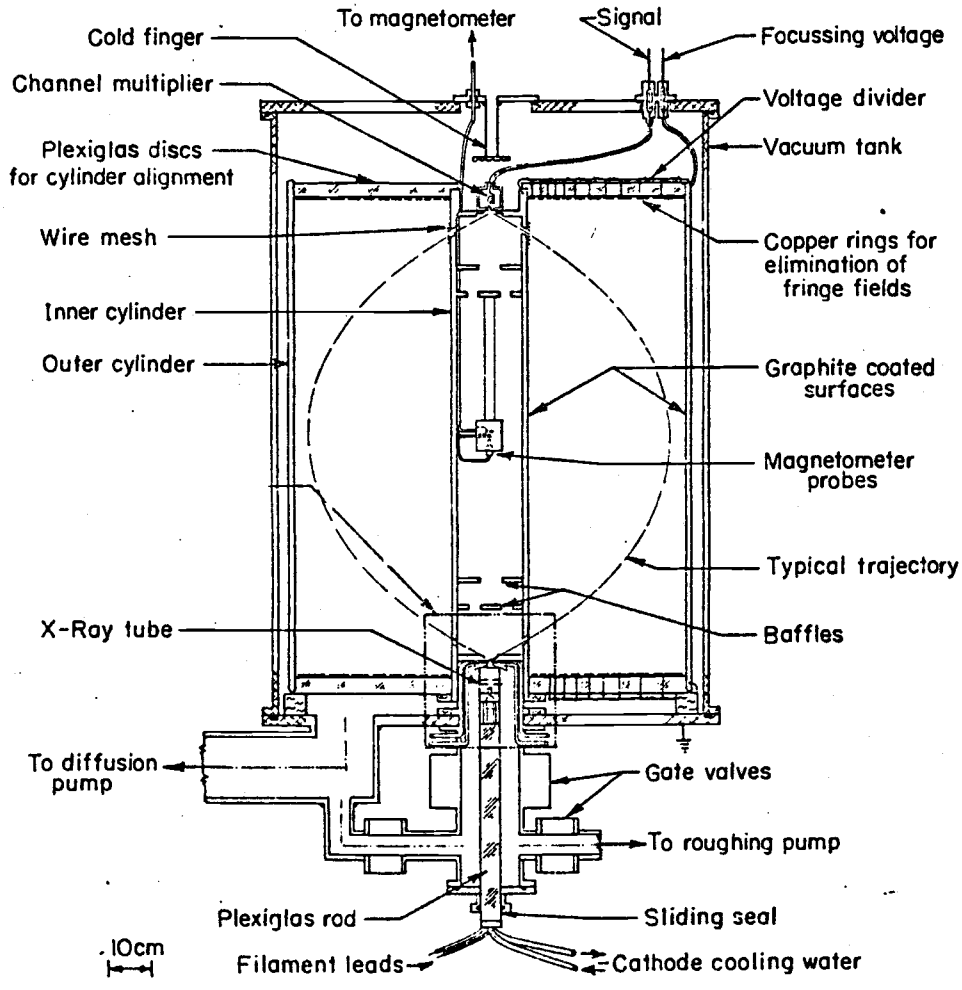

Figure 1. Oregon State University cylindrical electrostatic analyzer in cross section (from reference 30).

capable of operating at 80 watts with an aluminum anode and about 40 watts with a magnesium anode. For either material, the anode is held at 10kV. The power level attainable is limited by the rate of heat conduction away from the anode tip. At 80 watts and a sample gas pressure of approximately 10^{-2} Torr, typical count rates ranged from 3 to 10 counts per second for the compounds analyzed here.

The sample pressure was deliberately kept low in order to minimize energy-loss phenomena, which interfere with satellite observation (to be discussed in a later section). The low sample density resulted in counting times of 12 to 100 hours, depending on the X-ray intensity, the X-ray absorption cross section for the atom being investigated, and the number of atoms of interest per molecule.

For furan, pyrrole, and thiophen, a computerized scanning and data collecting system (known as PESCAN, designed by T. D. Thomas) was used. By interfacing the detector electronics with a PDP-9 computer, one may scan four different regions of the spectrum in a repetitive cycle, spending different amounts of time in each region if desired. In order to obtain the maximum amount of data for the $\pi \rightarrow \pi^*$ satellites, I have spent between 10 and 20 times more counting time in these regions than in the primary-peak and high-energy satellite regions. The region from 0 to 25 eV on the low kinetic energy side of the primary photoline was scanned for each spectrum. Also, accurate core ionization potentials

were obtained for the heterocyclics utilizing a neon calibration technique described elsewhere (33).

For the fluorinated hydrocarbons, both $\pi \rightarrow \pi^*$ and high-energy satellites were investigated in equal detail, using a Northern Scientific NS-600 multichannel analyzer to scan the 0 to 50 eV region on the low-kinetic energy side of the primary peak. Accurate core ionization potential shifts have been previously measured for these coupounds (34,35).

A Separately Pumped X-ray Chamber

In the original spectrometer design, the X-ray tube is not isolated from the rest of the spectrometer so that the sample gas being examined is present in the X-ray tube. This design feature frequently results in deterioration of the filament and coating of the anode and window to the point where X-ray intensity declines substantially. Running at 80 watts, typical X-ray tube lifetimes range from 24 hours for relatively unreactive gases to 6 hours for highly reactive gases. This drawback led our research group to develop a separate pumping system for the tube. In this new system, the chamber in which the X-ray tube is placed is isolated from the rest of the spectrometer by a modified top plate on the tube itself that seals the tube to the gas sample cell (see Figure 2). The system is pumped by a Varian M-4 diffusion pump providing a pressure of 2×10^{-5} Torr when the X-ray rube is degassed and operating at the

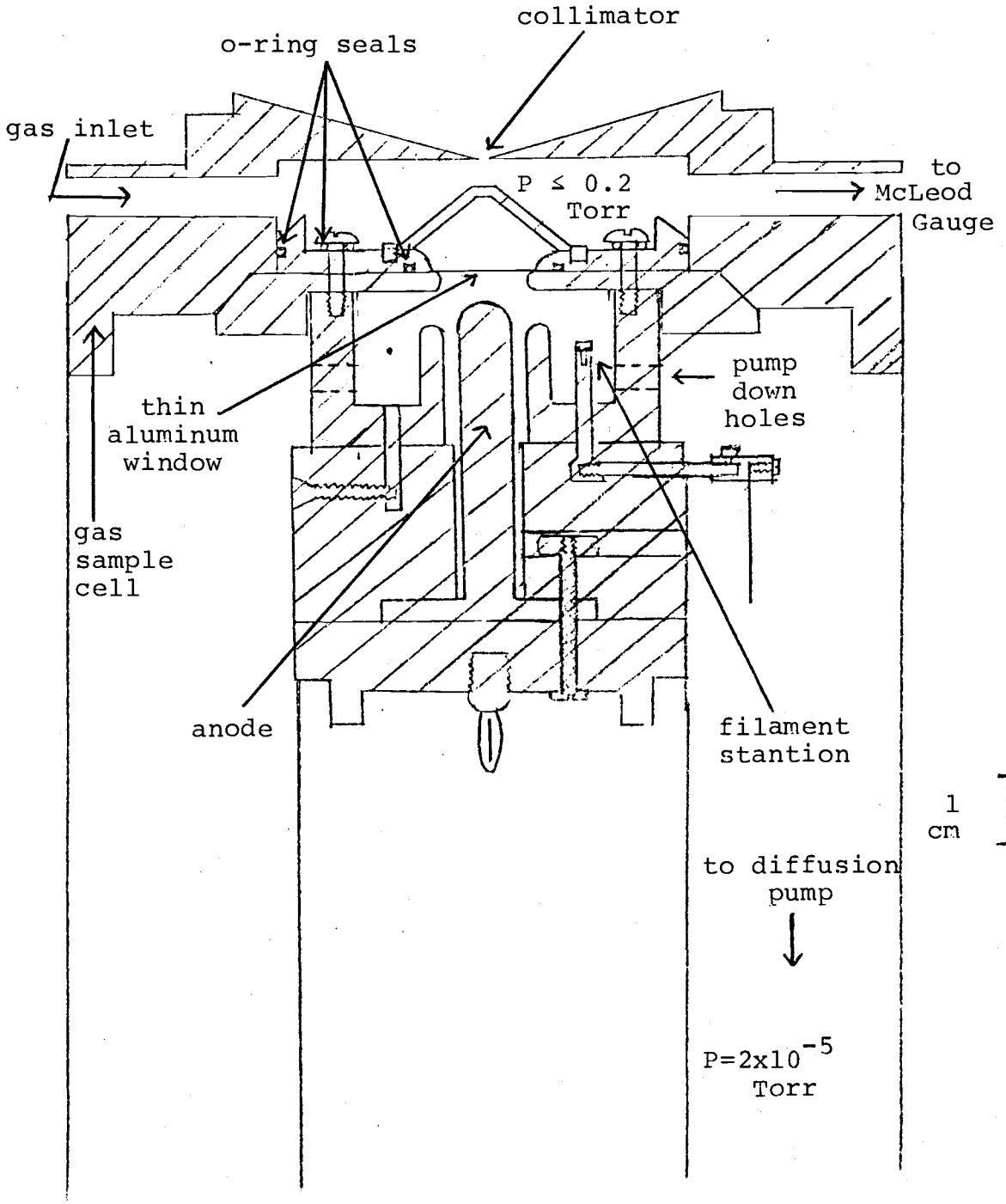

Figure 2. X-ray tube -- gas cell assembly.

present maximum power level of 80 watts. One may now keep the sample cell pressure as high as 0.2 Torr, while maintaining the X-ray tube at $2x10^{-5}$ Torr. Although the problem of tungsten deposition from the filament to the anode and window still eventually leads to X-ray attenuation, the life of the X-ray tube components has been increased to approximately 140 hours while the tube is running at 80 watts.

Problems of high voltage breakdown have been diminished. Before the separate pumping system was installed, discharges between the anode and the grounded cylindrical copper shield surrounding it occurred fairly frequently (36). If a discharge causes sufficient current to be drawn from the high voltage power supply, a protective overcurrent trip mechanism is activated, shutting down the power supply. In addition to immediately stopping progress on an experiment, the overcurrent trip frequently causes extraneous counts to appear in the data, reducing its quality. However, with the new pumping system, high voltage breakdown has occurred only when the tube is still outgassing after prior exposure to atmospheric pressure. Once outgassed and back down to $2x10^{-5}$ Torr, no breakdown has occurred even on one occasion when the anode tip accidently melted and flowed to within approximately 0.5mm of the grounded shield. Because of the absence of breakdown at 10 kV, the tube was run at 13 kV

during the last set of experiments performed for this work in order to achieve more efficient X-ray production (37).

The Elimination of Inelastic Scattering Structure

As photoelectrons leave the area to which the sample is confined, they may inelastically interact with molecules leading to valence shell excitations and energy-loss structure in the low kinetic energy region of the photoelectron spectrum. Such structure is highly undesirable in that it occurs in the same region as does satellite structure and makes satellite observation very difficult. The intensities of energy-loss peaks relative to the intensity of the elastic peak are proportional to the density of sample material whereas satellite intensities are not. Thus, the problem is much more acute in solid-phase studies than in gas-phase work. In the gas phase, one has the advantage of being able to keep the sample pressure very low in order to minimize inelastic scattering. Several workers (4,8,9) have taken spectra at a variety of pressures in order to determine which peaks are pressure dependent and then extrapolate to zero pressure to obtain the true shake-up spectrum. The following method is presented as an alternative to obtaining spectra at different pressures, and has been used to eliminate inelastic scattering from the satellite spectra measured here.

For a given satellite spectrum there are three contributions to the intensity: B_S, a background taken to be constant over the energy range of interest; $I_S(n)$, the true satellite intensity at channel n; and $I_L(n,P_S)$, the energy-loss intensity at channel n and sample pressure P_S. The observed satellite intensity for a given channel is the sum of these three terms.

$$I_{SO}(n,P_S) = B_S + I_S(n) + I_L(n,P_S) \qquad (3.1)$$

Similarly, at a given channel n in the inelastic electron scattering spectrum, the observed intensity is composed of background B_L and the inelastic scattering intensity as a function of channel number n and gas pressure P_L:

$$I_{LO}(n,P_L) = B_L + I_L(n,P_L) \ . \qquad (3.2)$$

For both spectra, the assumption is made that all intensity on the high kinetic energy side of the main peak is due to the constant background. An average over several channels at high kinetic energies is subtracted from the data at lower kinetic energies to provide spectra corrected for background.

The term $I_L(n,P_S)$ in Eq. 3.1 is related to the term $I_L(n,P_L)$ in Eq. 3.2 by a constant α such that for each channel n,

$$I_L(n,P_S) = \alpha I_L(n,P_L) \ . \qquad (3.3)$$

It is reasonable to expect that α is equal to P_S/P_L. However, because of the difficulty involved in measuring and controlling the pressure in the gas cell, α is determined empirically by the following method.

It is assumed that there is some channel in the low kinetic energy portion of the spectrum at which the energy-loss intensity is much greater than the satellite intensity. For the heterocyclic molecules, this is generally about 20-25 eV below the primary peak. Although one might expect satellites due to excitation from sigma orbitals in this region, the spectra are quite featureless and the intensity is either very weak or spread out over many channels. However in the case of the fluorinated hydrocarbons, the high-energy[1] satellite intensity is strong. There is either structureless intensity spread out over many channels as in the case of several of the carbon 1s spectra or a very broad, unresolved manifold of peaks that eventually comes down approximately to background as in the case of many of the fluorine 1s spectra. In both cases, it is common to find that the channel(s) where the ratio of observed energy-loss intensity to observed shake-up intensity is maximized is in the region between π and σ satellites.

---

[1]High-energy satellites refer to final states possessing a high-energy valence configuration relative to the ground state of the ion. Thus, such a state is at low kinetic energy relative to the primary peak, as governed by the conservation of energy equation (Eq. 1.1).

Once an appropriate channel, i, is selected at which the ratio of energy-loss intensity to satellite intensity is at a maximum, the assumption is made that the true shake-up intensity at that channel is approximately zero. In this case, Eq. 3.1 becomes

$$I_{SO}(i,P_S) - B_S = I_L(i,P_S) \quad . \tag{3.4}$$

Combining Eqs. 3.2 and 3.3 and inserting the result into Eq. 3.1, we obtain

$$\alpha = \frac{I_{SO}(i,P_S) - B_S}{I_{LO}(i,P_L) - B_L} \quad . \tag{3.5}$$

Having determined α, one may combine Eqs. 3.1, 3.2 and 3.3 to give an expression for the satellite intensity at channel n:

$$I_S(n) = I_{SO}(n,P_S) - B_S - \alpha[I_{LO}(n,P_L) - B_L] \quad . \tag{3.6}$$

It is to be noted that the method of determining α gives an upper limit because satellite intensity may need to be subtracted from the numerator in Eq. 3.5 in order to give the true value of α. The true satellite spectrum lies somewhere between the corrected and uncorrected spectra.

Data Analysis

All primary and low-energy $\pi \rightarrow \pi^*$ satellite peaks were least-squares fitted to Gaussian functions. In cases of

partially unresolved peaks, such as the primary carbon doublets in furan, pyrrole and 1,3,5-trifluorobenzene, a fitting program was used in which known area ratios can be held constant during the iterative process.

In order to estimate the intensity of the high-energy satellites, the total intensity from the onset of shake-up in the sigma orbitals to the low kinetic energy end of the spectrum was integrated numerically by summing the counts per channel corrected for background. The region generally spanned approximately 40 eV, starting at around 12 eV below the primary photoline. In addition to one-electron shake-up in the sigma orbitals, structure due to two or more electron shake-up and shake-off may be present in some of the spectra at these energies.

IV. SATELLITE STRUCTURE IN FURAN, PYRROLE, AND THIOPHEN

Gas-phase vs. Solid-phase Spectra

Pignataro and co-workers (10) have measured the satellite structure of furan, pyrrole and thiophen in the solid-phase. A comparison of their results with this work done in the gas-phase illustrates the advantages of making measurements in the gas phase. Figure 3 shows the spectra obtained in the gas phase and corrected for energy loss. In the central portion of each spectrum are three sets of data that were collected 10 times as long as the data in the outer regions. The top is the uncorrected satellite spectrum, the solid line at the bottom represents the normalized energy-loss spectrum, and the points in the middle show the corrected satellite spectrum. In general the correction is small. The uncorrected and corrected shake-up data have been smoothed using a 3-point smoothing routine. The carbon 1s spectra of furan and pyrrole and to a lesser extent the heteroatom spectra of these molecules show striking similarities between shake-up and energy-loss spectra. It is clear that even at the low sample pressure of $\sim 10^{-2}$ Torr, neglecting to properly normalize and subtract inelastic scattering from the shake-up data would lead to overestimates of the intensities. On the low kinetic energy side

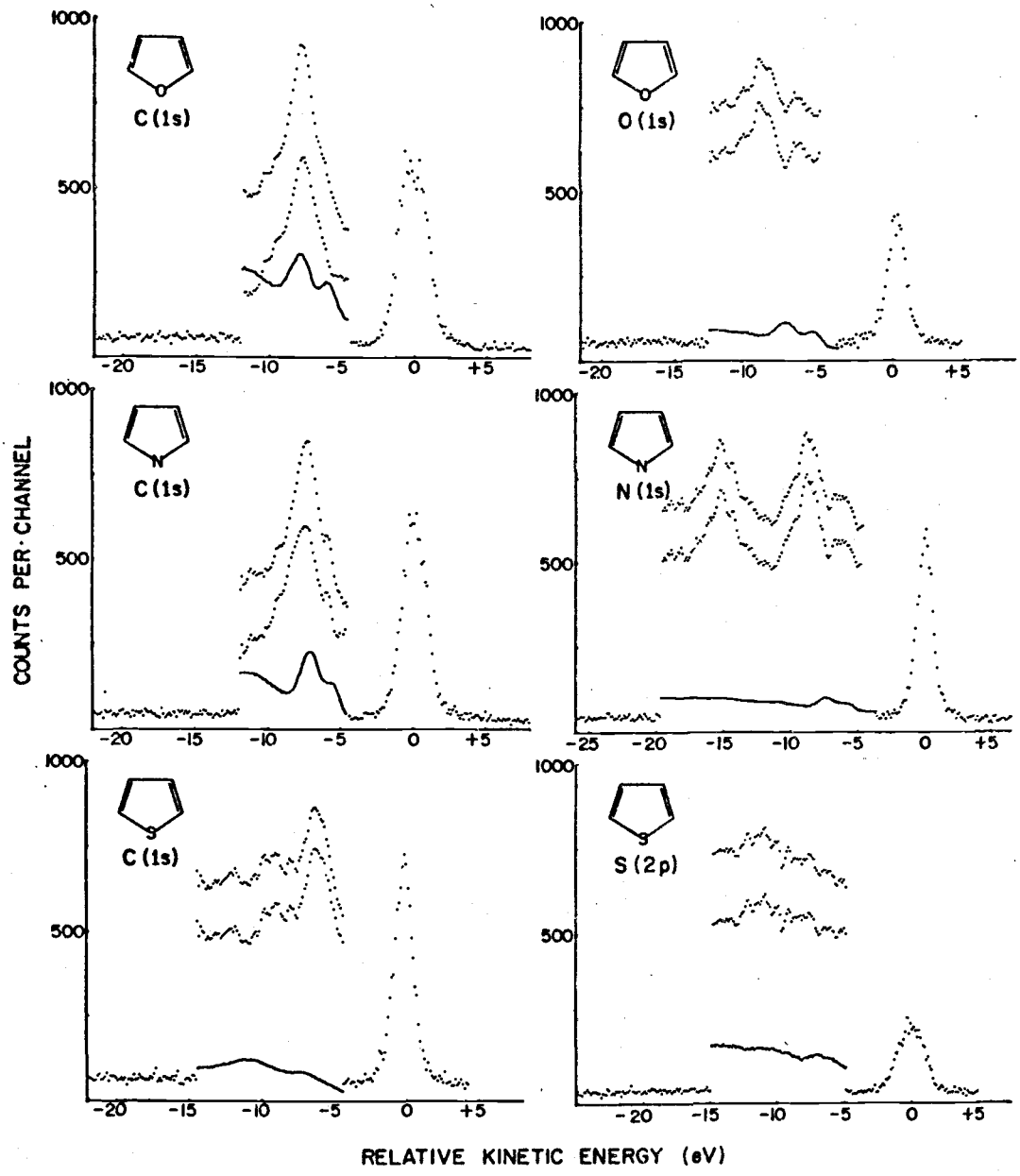

Figure 3. X-ray (AlKα) photoelectron spectra of furan, pyrrole, and thiophen.

of the solid-phase data the background rises rapidly, making it difficult to identify the satellite peaks or to determine their intensities accurately. The background on the low kinetic energy side of the gas-phase data is relatively low and flat.

The energies and intensities from both gas-phase and solid-phase spectra are listed in Table 2. The numbers listed are relative to the position and intensity of the primary photoline. There is generally good agreement between the two sets of data, but significant disagreements do exist.

The most striking discrepancy exists between the reported intensities of the carbon 1s satellite in furan. The intensity obtained from the solid-phase spectrum exceeds that from the gas-phase spectrum by nearly a factor of four. The gas-phase electron-impact data show a strong peak at nearly the same energy as that of the shake-up peak. Because of this result, the uncertainty involved in assigning an intensity to the shake-up peak in the solid-phase spectrum would be great. The agreement between solid- and gas-phase measurements for the carbon 1s spectra of pyrrole seems to be much better, although the problem of overlapping shake-up and energy-loss peaks exists in this case also.

If the intensity of a satellite peak is weak, it becomes very difficult to distinguish its presence from the high background and energy loss present in a solid-phase

Table 2. Experimental intensities and energies of shake-up satellites for the heterocyclic molecules.

Compound	Intensity (%) a	Intensity (%) b	Energy (eV) a	Energy (eV) b
Furan				
C(1s)	100		0	
	7.2	32	7.64(3)	7.7
O(1s)	100		0	
	0.4		6.7	
	2.8		9.17(5)	8.6
Pyrrole				
C(1s)	100		0	
	7.4	8	7.63(4)	7.2
N(1s)	100		0	
	0.5		6.5	
	3.6		8.74(4)	8.0
	3.4		15.06(6)	
Thiophen				
C(1s)	100		0	
	5.0	7	5.93(4)	5.7
	1.9		8.7 (1)	
S(2p)	100		0	
	3		11.1 (6)	7.5(5)

Numbers in parentheses give the estimated uncertainty in the last digit.

a. Gas phase, this work.

b. Solid phase, ref. 10.

spectrum. The additional weak peaks seen in the gas-phase spectra of oxygen 1s of furan, nitrogen 1s of pyrrole, and carbon 1s of thiophen are presumably obscured by inelastic scattering in the solid-phase spectra.

Comparison of Theory and Experiment

Table 3 contains the gas-phase satellite data and theoretical intensities and energies for π electrons obtained using CNDO/2 wave functions. The intensities and energies are relative to those of the primary photoline. Each calculated final state is labeled according to the π-orbital occupancy.

The neutral molecules all possess C_{2V} symmetry. Therefore, the molecular orbitals have been given symmetry labels corresponding to the irreducible representations of the C_{2V} point group in order to facilitate comparison of final states in different molecules. The ground state of the π system of the three molecules is typically

$$(1b_1)^2\ (2b_1)^2\ (1a_2)^2\ (3b_1)^0\ (2a_2)^0.$$

For core ionization on the C_2 axis (the heteroatom), the symmetry of the molecule is unchanged and the ground state configuration of the ion is the same as that of the molecule. The monopole selection rule allows only three transitions: $(1b_1 \rightarrow 3b_1)$, $(2b_1 \rightarrow 3b_1)$, and $(1a_2 \rightarrow 2a_2)$. Only the

Table 3. Comparison of experimental and theoretical results for the heterocyclic molecules.

Compound and Atom	Orbital [a]	Intensity (%)		Energy (eV)	
		b	c	b	c
Furan					
C(1s)	$(1a''2a''3a'')_{2,3}$	100	100	0	0
	$(1a''2a''4a'')_2$	13.6		9.8	
	$(1a''4a''3a'')_3$	5.8	7.2	12.7	7.64
	$(1a''4a''3a'')_2$	4.1		11.2	
O(1s)	$(1b_1 2b_1 1a_2)$	100	100	0	0
			0.4		6.7
	$(1b_1 3b_1 1a_2)$	4.8	2.8	15.1	9.17
Pyrrole					
C(1s)	$(1a''2a''3a'')_{2,3}$	100	100	0	0
	$(1a''4a''3a'')_2$	14.2		10.8	
	$(1a''2a''4a'')_2$	2.9	7.4	10.1	7.63
	$(1a''4a''3a'')_3$	8.2		12.2	
N(1s)	$(1b_1 2b_1 1a_2)$	100	100	0	0
			0.5		6.1
	$(1b_1 3b_1 1a_2)$	8.1	3.6	13.7	8.74
			3.4		15.06
Thiophen					
C(1s)	$(1a''2a''3a'')_{2,3}$	100	100	0	0
	$(1a''4a''3a'')_2$	11.0		10.4	
	$(1a''4a''3a'')_3$	6.7	5.0	9.7	5.93
	$(1a''5a''3a'')_3$	1.9	1.9	13.2	8.7
S(2p)	$(1b_1 2b_1 1a_2)$	100	100	0	0
	$(1b_1 3b_1 1a_2)$	2.0	3.	12.0	11.1

a. Subscripts outside the parenthesis refer to location of carbon in the ring. The heteroatom is 1.

b. Calculated

c. Experimental

second of these is predicted to have appreciable strength according to the calculation. The experimental intensities for the heteroatom K-shell spectra for furan and thiophen are only in moderate agreement with the prediction. The spectrum for pyrrole shows two satellites of approximately equal intensity in addition to one very weak one, and yet only one satellite is predicted. It is possible that the highest energy satellite is due to shake-up in the sigma orbitals. However, such a notion is merely conjecture and cannot be validated because the calculation for satellites involving sigma orbitals was not done for these molecules because of computer-size limitations. The other possibility is simply that the theory is not capable of predicting the correct number of satellites in all cases and is, therefore, of dubious value. The calculated intensities for the heteroatom spectra are, except for thiophen, about a factor of two higher than observed.

For core ionization off the C_2 axis (the carbons), the symmetry of the ion is reduced to C_s and the ground state configuration of the π electrons becomes

$$(1a")^2\ (2a")^2\ (3a")^2\ (4a")^0\ (5a")^0$$

The monopole selection rules allow six transitions between the occupied and unoccupied orbitals. Since there are two inequivalent carbons, 12 possible transitions exist. Only three of these are predicted to have intensity greater than

1%. For each molecule, the transitions (2a" → 4a"), with the core hole on either carbon site are predicted to be reasonably strong. For furan and pyrrole, core ionization of the carbon adjacent to the heteroatom is predicted to result in a relatively strong (3a" → 4a") transition. For thiophen the transition (2a" → 5a") is predicted to be greater than 1% when the carbon not adjacent to the heteroatom is ionized.

For the most part, the satellites are predicted to be so close to one another in energy as to be nearly unresolvable. The expected and observed result is that there should be one broad peak. For thiophen, however, there is experimental and theoretical evidence for a second, resolvable peak. The predicted intensities are, as for the heteroatom spectra, too high by a factor of two.

The predicted energies of the satellites, though qualitatively correct, are in general greater than the observed energies. As mentioned earlier, relaxation toward the valence hole in the shake-up state has been neglected in the theoretical treatment, making the excited ionic state essentially a Koopmans'-theorem state. For this reason, the predicted energies are in excess of the observed energies.

Qualitatively, the CNDO/2 wave functions give correct results. Satellites about 10 eV from the main peak with intensities about 10% of that of the main peak are predicted and observed. However, the theory fails to predict the

intensities, the trends in intensity from one compound to another, or (as in pyrrole) the number of major satellites. These results are in accord with those of Martin, Mills, and Shirley, who found that highly sophisticated wave functions were needed to give accurate predictions of shake-up in HF (8) and Ne (7). They are, however, in disagreement with the conclusions drawn by Clark and Adams in the usefulness of CNDO/2 wave functions for prediction of shake-up in pyridine and perfluoropyridine (11).[2] It is to be noted that the experiments of Clark and Adams were done with solid-phase samples, precluding correction for energy-loss. Therefore, overestimation of the shake-up intensity provides a possible explanation for the good agreement between theory and experiment; gas-phase results yield an intensity about a factor of two less than the predicted intensity for the nitrogen 1s spectrum of pyrrole.

Accurate Core Ionization Potentials

Core ionization potentials for furan, pyrrole, and thiophen were measured using a Ne calibration technique described by Thomas and Shaw (33). The results are listed in Table 4. $MgK\alpha_{1,2}$ radiation was used for the carbon 1s

[2]Calculation of the ($b_1 \rightarrow b_1^*$) shake-up transition intensity accompanying core ionization of nitrogen in pyridine done here reproduced the theoretical results of Clark and Adams, verifying inclusion of the factor of two in their calculation that is necessary to account for the double occupancy in the initial orbital.

Table 4. Core ionization potentials for the heterocyclic molecules (eV).

Compound	Core Ionization Potential	Splitting
Furan		
C(1s)	290.60(6) 291.81(6)	1.22(2)
O(1s)	539.95(4)	
Pyrrole		
C(1s)	289.96(7) 290.77(7)	0.81(8)
N(1s)	406.15(4)	
Thiophen		
C(1s)	290.61(4)	
S(2p3/2)	170.04(4)	1.22(3)
S(2p1/2)	171.25(5)	

Numbers in parentheses give the uncertainty in the last digit.

spectra of furan and pyrrole and the sulfer 2p spectrum of thiophen in order to enhance the resolution of the closely spaced doublets. Each entry is an average of either two or three separate experiments. The doublets were resolved using a fitting routine in which area ratios were held constant.

The effect of decreasing electronegativity of the heteroatom on the splitting between inequivalent carbons is apparent as one goes down the series. The splittings reported here are in excellent agreement with those of Gelius et al. (38), also measured in the gas-phase. The absolute energies reported here differ by tenths of an eV with those that they have reported.

V. SATELLITE STRUCTURE IN FLUORINATED HYDROCARBONS

Experimental Results

Figures 4, 5 and 6 show the corrected satellite and inelastic scattering spectra for several fluorinated hydrocarbons. At 0 eV relative kinetic energy is the primary photoline. In the low kinetic energy region are the energy-loss data, represented by a solid line, and the shake-up spectra corrected for inelastic scattering, represented by a point plot. The satellites and energy-loss spectra have both been expanded by the indicated factor in order to display their structure. All the spectra except that for the fluorine 1s ionization in vinyl fluoride show a pronounced peak at slightly less than 10 eV, which is well separated from a broad region of high-energy satellites. For those molecules that contain chemically inequivalent carbon atoms, there is evidence for unresolved low-energy satellites in the carbon 1s spectra. In general, the fluorine 1s spectra appear to contain more structure in the high-energy region than do the carbon 1s spectra, which are relatively flat.

Ethylene (4) and benzene (9) have previously been examined in the gas-phase. The results for ethylene and those for the low-energy satellites of benzene reported here are in fairly good agreement with those previously reported. A comparison is provided in Table 5. However,

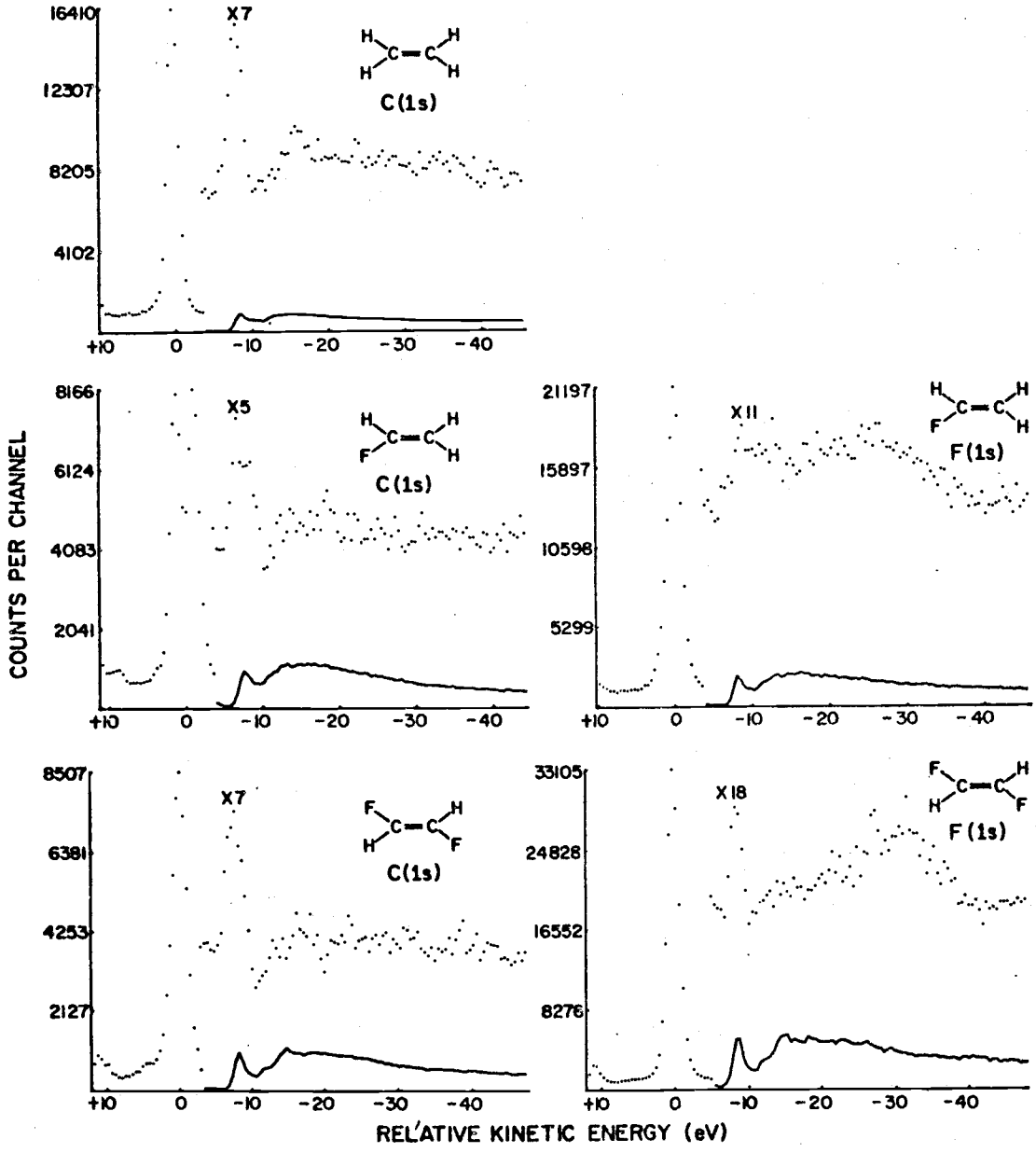

Figure 4. X-ray (AlKα) photoelectron spectra of ethylene, vinyl fluoride, and trans-1,2-difluoroethylene.

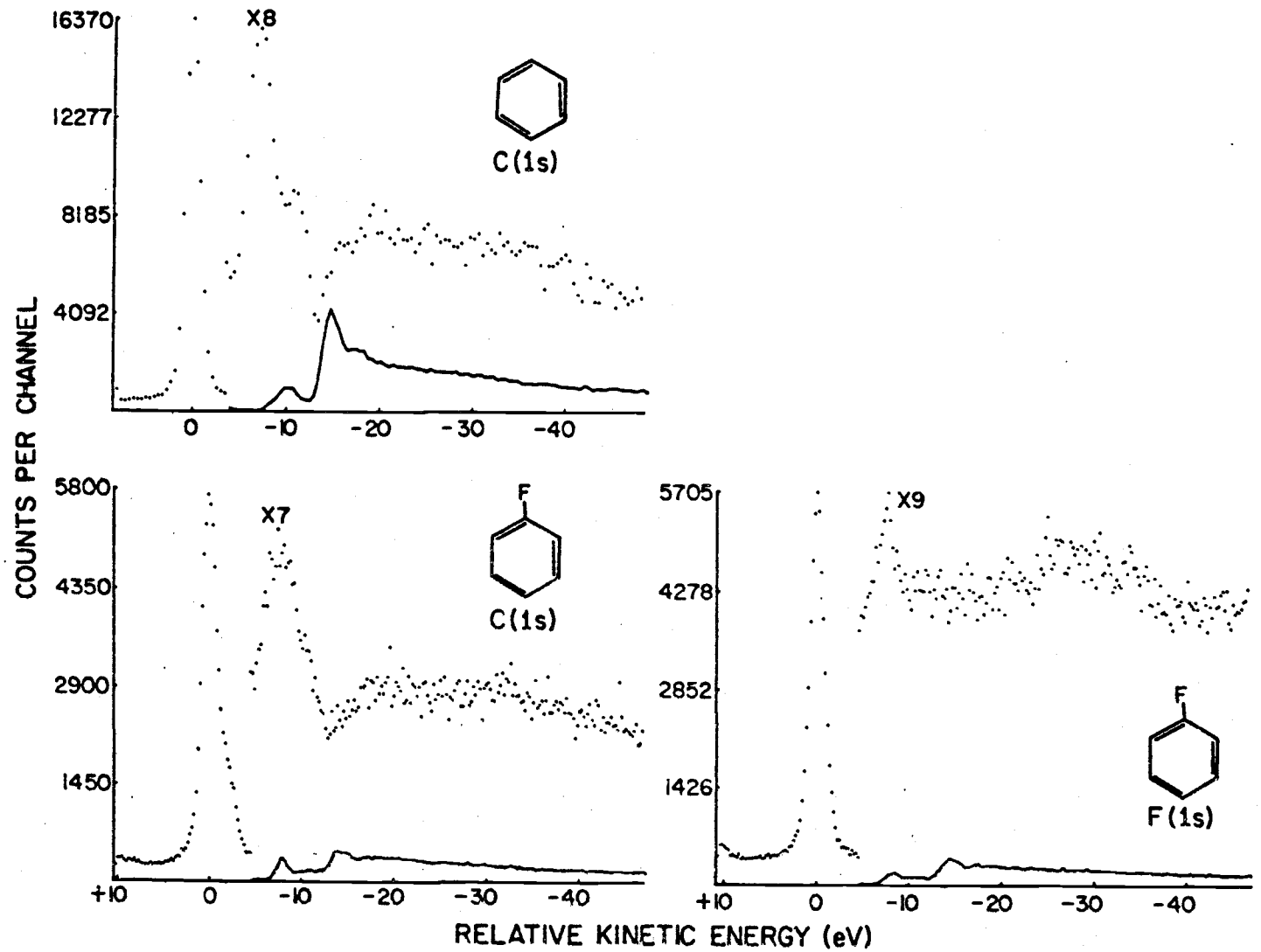

Figure 5. X-ray (AlKα) photoelectron spectra of benzene and fluorobenzene.

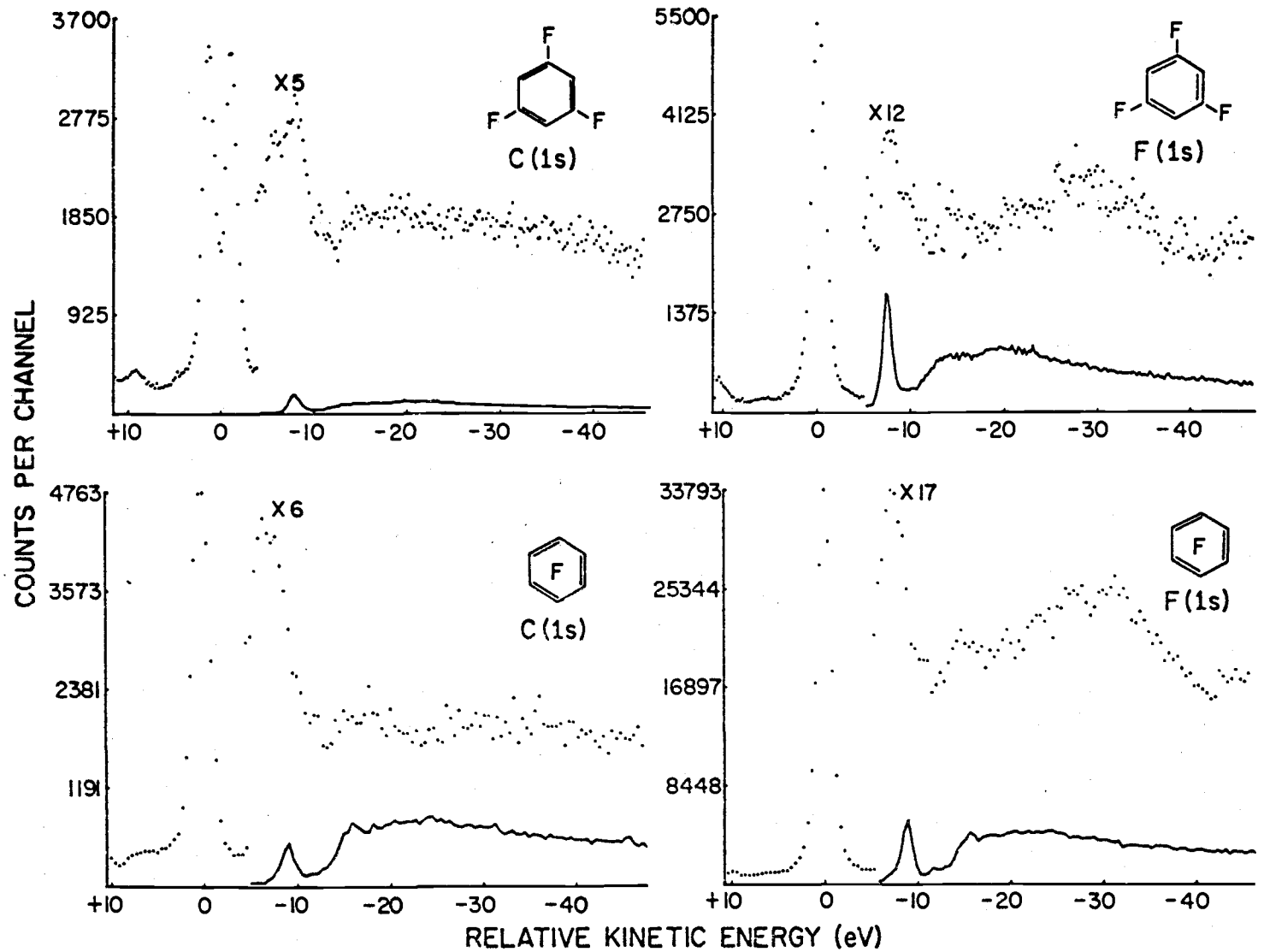

Figure 6. X-ray (AlKα) photoelectron spectra of 1,3,5-trifluorobenzene and hexafluorobenzene.

Table 5. Comparison of satellite intensities and energies using two methods of energy-loss correction for ethylene and benzene in the gas-phase.

Compound	Intensity (%)		Energy (eV)	
	a	b	a	b
Ethylene				
C(1s)	100		0	
	8.1	9.7	8.46(10)	8
	27	28	12-50	10-50
Benzene				
C(1s)	100	100	0	0
	13.2	10.5	7.18(8)	7.0
	3.4	2.5	10.9(1)	11.0
	30	--	13-50	--

Numbers in parentheses give the estimated uncertainty in the last digit.

a. Gas-phase, this work. Inelastic scattering removed by subtraction of normalized energy-loss spectra.

b. Gas-phase, references 4 and 9. Inelastic scattering removed by measuring at different pressures and extrapolating to zero pressure.

for benzene, high-energy intensity amounting to about 30% of that of the primary line remains in this work after energy-loss correction. Ohta, Fujikawa, and Kuroda observed weak bands in the high-energy region but were unable to dismiss the possibility that they originated from inelastic scattering phenomena (9).

Comparison of Theory and Experiment

Tables 6 and 7 show the comparison of experimental and theoretical (CNDO/2) results for the fluorinated hydrocarbons. In the case of the ethylene and the fluorinated ethylenes, all possible shake-up states involving single-electron excitations were calculated. Because of computer-size limitations, the calculations for benzene and the fluorobenzenes were restricted to shake-up states involving single π-electron excitations.

This set of molecules is not characterized by a single symmetry. Therefore, rather than assign irreducible representations to the molecular orbitals from the various point groups represented, the orbitals are designated simply as σ or π orbitals. The number preceding the σ or π designation refers to the order of its energy relative to the energies of the other orbitals of the same symmetry (σ or π). For example, 1σ and 1π refer to the lowest energy σ and π orbitals of the valence set.

Table 6a. Comparison of experimental and theoretical results for ethylene.

Atom	Shake-up Transition	Intensity (%) Calc.	Intensity (%) Exp.	Energy (eV) Calc.	Energy (eV) Exp.
C(1s)	$1\pi \rightarrow 2\pi^*$	8.8	8.1	13.9	8.46(10)
	$5\sigma \rightarrow 9\sigma^*$	2.2		17.2	
	$4\sigma \rightarrow 8\sigma^*$	1.4		19.8	
	$3\sigma \rightarrow 7\sigma^*$	0.9	27	24.5	12-50
	$2\sigma \rightarrow 6\sigma^*$	2.1		26.0	
	$1\sigma \rightarrow 6\sigma^*$	1.2		37.6	
	Total σ	7.8			

Table 6b. Comparison of experimental and theoretical results for vinyl fluoride.

Atom	Shake-up Transition	Intensity (%) Calc.	Intensity (%) Exp.	Energy (eV) Calc.	Energy (eV) Exp.
C(1s)+	$2\pi \rightarrow 3\pi^*(1)$[a]	9.6	13.1	14.7[b]	8.78(9)[b]
	$2\pi \rightarrow 3\pi^*(2)$	9.9		12.8	
	$1\pi \rightarrow 3\pi^*(1)$	1.2	20	20.5[b]	11-50
	$7\sigma \rightarrow 11\sigma^*(1)$	2.3		21.7[b]	
	$5\sigma \rightarrow 10\sigma^*(1)$	1.1		24.0[b]	
	$4\sigma \rightarrow 9\sigma^*(1)$	1.1		26.9[b]	
	$3\sigma \rightarrow 8\sigma^*(1)$	2.5		27.7[b]	
	$3\sigma \rightarrow 8\sigma^*(2)$	1.1		25.5	
	$2\sigma \rightarrow 8\sigma^*(2)$	1.4		36.8	
	Total High-energy	10.7			
F(1s)	$7\sigma \rightarrow 8\sigma^*$	6.1	23	11.4	7-50
	$2\pi \rightarrow 3\pi^*$	3.5		14.4	
	$6\sigma \rightarrow 8\sigma^*$	4.7		15.4	
	$5\sigma \rightarrow 8\sigma^*$	2.2		18.8	
	$4\sigma \rightarrow 8\sigma^*$	4.8		23.7	
	$3\sigma \rightarrow 8\sigma^*$	6.1		25.1	
	$1\pi \rightarrow 3\pi^*$	1.1		27.8	
	$1\sigma \rightarrow 8\sigma^*$	3.0		52.4	
	Total	31.5			

a. Numbers in parentheses refer to location of the carbon. One is bonded to the fluorine.

b. Relative to carbon 2 (with the lower binding energy).

+. The carbon splitting is predicted to be 2.2 eV by the CNDO/2 approximation. The experimental splitting is 2.43(3) eV.

Table 6c. Comparison of experimental and theoretical results for trans 1,2-difluoroethylene.

Atom	Shake-up Transition	Intensity (%) Calc.	Intensity (%) Exp.	Energy (eV) Calc.	Energy (eV) Exp.
C(1s)	$3\pi \rightarrow 4\pi^*$	11.9	8.7	11.8	7.15(9)
	$9\sigma \rightarrow 12\sigma^*$	1.3		16.2	
	$1\pi \rightarrow 4\pi^*$	1.0		18.8	
	$6\sigma \rightarrow 11\sigma^*$	0.8	28	24.0	11-50
	$4\sigma \rightarrow 10\sigma^*$	1.4		25.5	
	$3\sigma \rightarrow 10\sigma^*$	1.3		32.8	
	Total High-energy	5.8			
F(1s)	$3\pi \rightarrow 4\pi^*$	4.0	1.1	13.1	8.09(10)
	$8\sigma \rightarrow 10\sigma^*$	6.6		16.3	
	$4\sigma \rightarrow 10\sigma^*$	2.0		23.5	
	$5\sigma \rightarrow 10\sigma^*$	11.4	20	23.7	11-50
	$1\pi \rightarrow 4\pi^*$	0.9		28.2	
	$1\sigma \rightarrow 10\sigma^*$	3.1		52.2	
	Total High-energy	24.0			

Table 7a. Comparison of experimental and theoretial results for benzene and fluorobenzene.

Compound and Atom	Shake-up Transition	Intensity (%) Calc.	Intensity (%) Exp.	Energy (eV) Calc.	Energy (eV) Exp.
Benzene			13.2		7.18(8)
C(1s)	$2\pi \rightarrow 4\pi^*$	10.4	3.4	10.0	10.9(1)
	High-energy	d	30	d	13-50
Fluorobenzene					
C(1s)+	$4\pi \rightarrow 5\pi^*(4)$ [a]	4.1		10.5	
	$3\pi \rightarrow 5\pi^*(4)$	6.6	16.7	10.8	7.68(12)
	$3\pi \rightarrow 5\pi^*(3)$	8.5		11.5	
	$3\pi \rightarrow 5\pi^*(2)$	10.0		12.1	
	$4\pi \rightarrow 6\pi^*(1)$	2.7[b]	1[c]	14.9[b]	10(2)[c]
	High-energy		28	d	12-50
F(1s)	$3\pi \rightarrow 5\pi^*$	3.6	2.5	11.9	7.4(1)
	High-energy	d	22	d	10-50

a. Numbers in parentheses refer to location of the carbon. One is bonded directly to the fluorine.

b. Relative to carbons 2, 3, and 4.

c. Relative to centroid of unresolved carbon peak.

d. Not calculated.

+ The predicted carbon splitting between carbon 1 and the combination of the others is 2.0 eV. The experimental result is 2.04(3) eV (34).

Table 7b. Comparison of experimental and theoretical results for 1,3,5-trifluorobenzene.

Atom	Shake-up Transition	Intensity (%) b	Intensity (%) c	Energy (ev) b	Energy (ev) c
C(1s)$^{+}$	$5\pi \rightarrow 7\pi^*(1)$[a]	11.0	11.5	10.3	6.8
	$4\pi \rightarrow 7\pi^*(1)$	2.8	e	13.8	e
	$5\pi \rightarrow 7\pi^*(2)$	9.7	5.3	11.3	7.0
	$4\pi \rightarrow 7\pi^*(2)$	2.6	1.4	14.7	11.9
	High-energy	d	11	d	14-50
F(1s)	$5\pi \rightarrow 7\pi^*$	2.9	1.1	11.2	7.4
	$4\pi \rightarrow 7\pi^*$	1.5	0.5	16.3	9.4
	$1\pi \rightarrow 7\pi^*$	1.3	e	28.9	e
	High-energy	d	27	d	12-50

a. Numbers in parentheses refer to location of the carbon. One is bonded directly to the fluorine.

b. Calculated; relative to ground ionic state with a core hole at the indicated carbon.

c. Experimental; relative to ground ionic state with a core hole at the indicated carbon.

d. Not calculated.

e. Not observed. Possibly buried in high-energy intensity.

+ The carbon doublet splitting is predicted to be 2.66 eV. The experimental result is 2.46(16) (34).

Table 7c. Comparison of experimental and theoretical results for hexafluorobenzene.

Atom	Shake-up Transition	Intensity (%) Calc.	Intensity (%) Exp.	Energy (eV) Calc.	Energy (eV) Exp.
C(1s)	$8\pi \rightarrow 10\pi^*$	12.0	12.3	9.9	7.0(1)
	High-energy	a	11	a	13-50
F(1s)	$8\pi \rightarrow 10\pi^*$	3.6	4.1	10.4	7.26(9)
	$7\pi \rightarrow 10\pi^*$	1.4		14.5	
	High-energy	a	33	a	13-50

a. Not calculated.

In general, there seems to be somewhat better agreement between theory and experiment for the π-orbital satellites in this series than in the series of heterocyclics. In most cases, intensities are in closer agreement with experimental values than was found for furan, pyrrole, and thiophen. In all cases except the fluorine 1s spectrum of vinyl fluoride, the theory predicts that the low-energy $\pi \rightarrow \pi^*$ satellites are well separated from the high-energy satellites, in good agreement with experiment. In cases where inequivalent carbons are present, the theory predicts two or more closely spaced π-orbital satellites. As mentioned earlier, vibrational broadening frequently keeps these peaks from being experimentally resolvable. For instance, the carbon 1s spectrum of vinyl fluoride indicates a low-energy doublet satellite that is experimentally only partially resolved. The CNDO/2 approximation predicts two peaks resulting from the $(2\pi \rightarrow 3\pi^*)$ transition accompanying core ionization of each carbon separated by about 2 eV. Similarly, in the case of the carbon 1s spectrum of fluorobenzene, there is experimental evidence for unresolved low-energy satellites with a shoulder on the high-energy side. The theory predicts four closely-spaced π-orbital satellites resulting from core ionization of C(2), C(3), and C(4) [$4\pi \rightarrow 5\pi^*$ (4), $3\pi \rightarrow 5\pi^*$ (4), $3\pi \rightarrow 5\pi^*$ (3), $3\pi \rightarrow 5\pi^*$ (2)], and a weaker satellite on the high-energy side of these four [$4\pi \rightarrow 6\pi^*$ (1)]. Finally, major and minor low-energy satellites are predicted for core

ionization of C(1) [$4\pi \rightarrow 7\pi^*$ (1) and $5\pi \rightarrow 7\pi^*$ (1)] and C(2) [$4\pi \rightarrow 7\pi^*$ (2) and $5\pi \rightarrow 7\pi^*$(2)] in the 1,3,5-trifluorobenzene; three of these four peaks are observed.

Qualitative success seems to have been achieved in predicting the low-energy $\pi \rightarrow \pi^*$ satellites in the fluorine 1s spectra of these molecules. In general, the correct number of peaks are predicted. In the case of hexafluorobenzene, two π-orbital satellites are predicted and one peak with a slight asymmetry on the high-energy side is observed.

Another interesting feature found in the experimental data is that the ratio of high-energy to low-energy ($\pi \rightarrow \pi^*$) satellite intensity is always larger in the fluorine 1s spectrum than in the carbon 1s spectrum for a given compound. The theory also predicts this trend, but only with qualitative agreement with experiment.

The predicted high-energy intensity is, in general, far below the observed value for the carbon 1s spectra and somewhat in excess of experimental results for the fluorine 1s spectra. Three potential sources of error in the method of calculation may be put forth in an attempt to account for this discrepancy. They are the failure to calculate multiple excitation probabilities, the inaccuracy of CNDO/2 wave functions due to the limited basis set and neglect of configuration interaction, and the assumption that the unoccupied orbitals from the equivalent-cores calculation are good approximations to the excited-state orbitals.

Recall that the calculations performed here include only single-electron excitations from the ground state configuration of the equivalent-cores ion. Thus, one is tempted to rationalize the lack of agreement between theory and experiment for the high-energy carbon 1s satellites on the basis of neglect of multielectron shake-up in the calculations, which, according to this way of thinking, would be unimportant in accounting for fluorine 1s high-energy satellite intensity. However, the sum of all intensities involving one-electron σ and π-orbital shake-up events and the intensity to the ground state of the ion account for at least 98% of the total calculated intensity in both carbon and fluorine hole-states for ethylene, vinyl fluoride, and trans-1,2-difluoroethylene. If multielectron effects were important in accounting for the observed intensity theoretically, one would expect the calculated intensity involving only one-electron excitations to be substantially less than 100%, the remainder being due to multielectron shake-up. However, this is not the case, implying that something else is wrong with the theory. It should be noted that multiple shake-up and shake-off may <u>in reality</u> account for some of the high-energy intensity, but within this basis set, such effects are not important; nearly 100% of the calculated intensity is due to one-electron shake-up among σ and π orbitals. If one were to expand the basis set, it is

possible that such multielectron transitions and shake-off would add intensity to the theoretical spectra.

A second possible explanation is the neglect of anything beyond the absolute minimum of valence atomic orbitals in the basis set for the CNDO/2 calculations. It may be argued that excited carbon hole-states of these molecules require Rydberg orbitals in the basis set for an accurate description whereas excited fluorine hole-states do not. One of the hopes for successful application of the CNDO/2 approximation to these molecules was that delocalization over many atoms would alleviate the need to extend beyond a valence basis set in describing the excited states. Is the apparent lack of agreement between theory and experiment for the carbon 1s spectra an indication of the need for a more complete basis set? Any improvement of the basis set would increase the quality of the calculation. However, there is no a priori reason why carbon 1s excited ionic states should require a better basis set than those of fluorine for a given molecule.

The neglect of configuration interaction (CI) could also be a source of inaccuracy in the carbon hole-state wave functions. Martin and Shirley (7) have shown in the case of Ne that extensive CI in both initial and final states is necessary to bring calculated intensities up to experimental values. The additional configurations in both states open up new "avenues" for populating the excited state that would not

be available if only the parent configurations were utilized. Again, the inclusion of CI can only improve a calculation, but to maintain that carbon 1s ionic states for a given molecule need to be correlated more than fluorine 1s ionic states of the same molecule is difficult to defend.

In addition to the approximate nature of the CNDO/2 method and the shortcomings mentioned above, there is one other feature of the calculation method that may be a root cause of some or all of the discrepancies noted in this work. The excited valence electron in a shake-up state is really moving in the field an N-2 electron core. In these calculations, however, the assumption has been made that the unoccupied eigenvectors from the equivalent-cores calculation are good approximations to the excited-state orbitals. In other words, the excited electron is treated as if it were moving in the field of an N-1 electron core. Martin, Mills, and Shirley (8) found that this approximation is a poor one when trying to construct accurate excited states by one-electron excitations from the reference configuration of the HF^+ core hole-state.

Finally, it should be noted that the CNDO/2 calculations done for this work have been unable to reproduce the calculated results given by others for ethylene and benzene. In the case of ethylene, I calculate higher intensity for π-orbital shake-up and much lower intensity for σ-orbital shake-up than do Carlson and co-workers (4). They have

apparently used Eq. 2.9 for some of their calculations (4) (and, consequently unnormalized wave functions) rather than Eq. 2.10, which is consistent with the CNDO/2 assumptions.

If in using Eq. 2.9, one is careful to include only the true values of atomic overlaps between orbitals of an atom and its equivalent-cores species, the molecular orbitals remain normalized. However, such integrals typically range from 0.94 to 0.99 in value. Therefore, substituting them for unity results in very small changes in the calculated intensity. Ohta, Fujikawa, and Kuroda report 5.3% for the intensity for the $2\pi \rightarrow 4\pi^*$ transition in benzene, calculated using CNDO/2 wave functions (9). The result obtained using Eq. 2.15 with CNDO/2 determinantal wave functions is 10.4%, approximation twice their value. They do not indicate, however, whether they have included the factor of two necessary to account for the number of electrons in the initial valence orbital.

VI. CHARGE REARRANGEMENT DURING PHOTOIONIZATION

Introduction

The satellite bands present in core-level photoelectron spectra have traditionally been interpreted in terms of some sort of charge rearrangement model. For atoms, the orbital description of excited ionic states involves transfering an electron from an occupied valence orbital to a virtual or continuum state (2). For transition metal complexes, low-energy satellites are frequently rationalized in terms of ligand-to-metal or metal-to-ligand charge transfer models (5, 22). In the case of other inorganic solids such as certain halides and oxides of copper (39), a valence-to-conduction band charge transfer model has been proposed to account for observed satellites. In some cases, interpretations have been made almost entirely on a phenomenological basis; in others, recourse to theoretical calculations has been made to aid in understanding the observations. An example of the former is the interpretation given by Pignataro and co-workers for the satellite spectra of furan, pyrrole, and thiophen in the solid-phase (10). They observed that the energy separation between the low-energy satellite and the primary peak was greater in the heteroatom spectra than in the carbon spectra and concluded that the shake-up process involves charge transfer from the hetero-

atom to the ring. Such an interpretation follows because if the initial valence orbital is primarily heteroatomic in character, it is preferentially stabilized by core ionization of the heteroatom and the transition energy will increase relative to the same transition in the neutral molecule. Similarly, the final valence orbital, being delocalized on the ring carbons, is preferentially stabilized by ionization of any of the carbons, lowering the transition energy relative to that in the neutral species. According to this model, charge is transferred away from the hole in the shake-up state when the heteroatom is core-ionized and toward the hold when the carbon is core ionized.

The ultimate test of such empirically-based interpretations comes not only from agreement with experimental results but also from compatibility with theoretical charge distributions for the molecule and various ionic states. The CNDO/2 wave functions, though of little quantitative value in accounting for either intensities or energies of satellites, can still provide qualitative information on how charge rearranges when the valence electrons are excited.

Charge Rearrangement in the Heterocyclic Molecules

Changes in the Mulliken charge in going from the ground ionic state to the important shake-up states are listed in Appendix B for furan, pyrrole, and thiophen. Values are given in units of 0.0le; a negative value associated with a

particular atom means that electrons leave the atom during the excitation. These numbers, derived using CNDO/2 wave functions, are based on π-electron populations for the various atoms. The results for the three molecules, though different in detail, are similar in overall pattern; all the major features can be seen in furan alone. Thus, the change in π-electron population at each atom when the core-ionized species is excited from its valence ground state to the indicated excited state is shown in Figure 7. In each case, the atom that has been core ionized is represented by its equivalent-cores species.

The most noticeable charge transfer is away from the heteroatom to some of the ring carbons (at least 0.1e), in agreement with the previous interpretation (10). This phenomenon occurs in the formation of the lowest three shake-up states in Figure 7 and in 9 of the 12 important states calculated. A second feature, seen in the first, third, and fourth drawings of Figure 7 is significant (at least 0.1e) charge transfer away from the core-ionized atom in populating certain excited ionic states. This phenomenon, which has not been previously discussed, occurs in 10 of the 12 shake-up states considered. Finally, for two of the calculations (top drawing) there is indication of charge transfer, not only from the core-ionized atom located in position two, but also from the carbon located in position four.

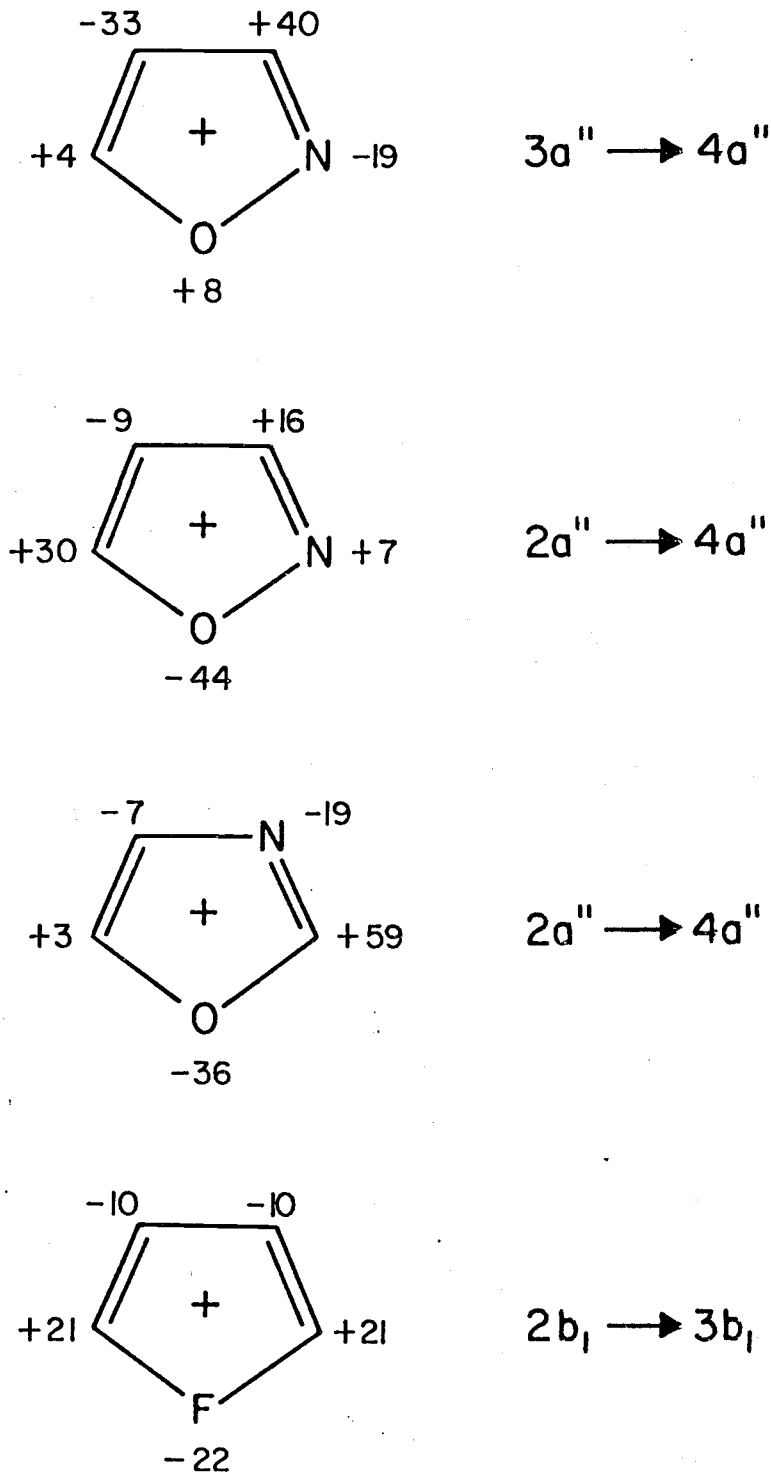

Figure 7. Change in electron population (in units of 0.01e) for core-ionized furan when the indicated valence excitation takes place. The core-ionized atom has been replaced by the appropriate equivalent-cores species.

The first of these is easily understood. In the absence of the perturbation due to the core hole, the low-lying excited states of the ion would be essentially those of the neutral molecule. The lowest of these corresponds to excitation of a $2b_1$ electron to a vacant $3b_1$ orbital. In furan, this transition involves the transfer of about 0.4e from the oxygen to the carbons. One might expect, therefore, that a shake-up transition will, to first order, involve a similar charge transfer. This result is seen in the calculations. The perturbation due to the presence of the core hole is also readily explained. The Koopmans'-theorem state, or unrelaxed ion, must be described as a linear combination of the ground and excited states of the relaxed ion. In the notation of Chapter II,

$$\Psi_{KT}(N-1) = \sum_{j=1}^{\infty} C'_j \Psi'_j(N-1) \qquad (4.1)$$

where the prime indicates eigenstates of the ionic Hamiltonian. The expansion coefficients are the scalar products $\langle \Psi'_j(N-1) \mid \Psi_{KT}(N-1) \rangle$ whose squares equal the probabilities of formation of the various states of the ion. If the ground ionic state, $\Psi'_o(N-1)$, has a charge distribution shifted in a given direction from that of the neutral molecule (or Koopmans'-theorem state of the ion), then the important excited states of the ion must have charge distributions shifted in the opposite direction from that of the ground ionic state. For example, consider oxygen 1s photoionization in

formaldehyde. Because of its higher electronegativity value, oxygen has a higher electron density than does carbon in the molecular ground state. Upon core ionization, extra-atomic relaxation toward the oxygen in the ground ionic state causes the charge distribution to be even more lopsided. This effect is illustrated in Figure 8, which shows atomic charges based on CNDO/2 wave functions. However, when the $\pi \rightarrow \pi^*$ shake-up state is populated (experimentally, in about 7% of all photoemission events), there is substantial charge transfer from the oxygen toward the carbon, also shown in Figure 8. There is only one satellite present in the oxygen 1s spectrum of formaldehyde (26), which has been assigned as the $\pi \rightarrow \pi^*$ shake-up state. Therefore, a linear combination of the wave functions for the ground ionic state and the π-orbital shake-up state is sufficient to describe Ψ_{KT}.

The remaining type of excitation is not simply explained. The symmetry of the original molecule has been changed by core ionization, with the result that there is no correspondence between the orbitals of the ion and the orbitals of the molecule.

These results show that, while the energy levels of the core-ionized species bear a resemblance to those of the neutral molecule, this resemblance is strongly modified by the rearrangement of charge caused by the core-ionization and, in some cases, by the lowering of the molecular symmetry.

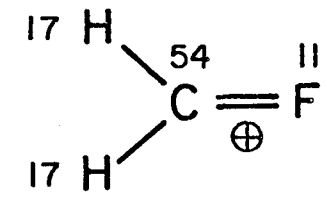

GROUND IONIC STATE

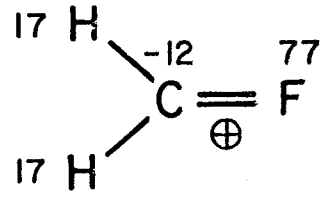

$\pi \rightarrow \pi^*$ SHAKE-UP STATE

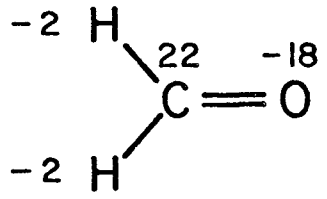

GROUND MOLECULAR STATE

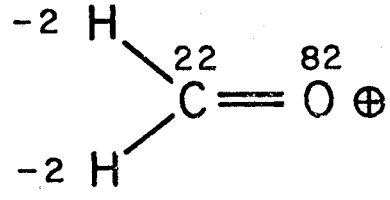

KOOPMANS' THEOREM STATE

Figure 8. CNDO/2 Mulliken charges (in units of 0.01e) for formaldehyde in the ground molecular, Koopmans'-theorem, ground ionic, and $\pi \rightarrow \pi^*$ shake-up states accompanying oxygen core ionization. The core-ionized oxygen is represented by its equivalent-cores species, fluorine.

In conclusion, it should be noted that no one simple interpretation such as heteroatom-to-ring charge transfer can describe all mechanisms of excited-state population. Rather, the charge rearrangement process is a highly complex one, involving several different directions of charge flow in the sample.

Charge Rearrangement in the Fluorinated Hydrocarbons

Appendix B contains the changes in atomic charge in going from the ground ionic state to the important shake-up states for ethylene, vinyl fluoride, trans-1,2-difluoroethylene, benzene, fluorobenzene, 1,3,5-trifluorobenzene, and hexafluorobenzene. The charges are derived separately for σ and π Mulliken populations using CNDO/2 wave functions, and are listed as such. Several interesting features appear in these calculations.

First, and perhaps most striking, is the migration of charge (at least 0.1e) from at least one of the fluorines in the formation of shake-up states accompanying carbon core-ionization. This phenomenon occurs in 11 of the 15 important π shake-up states and in 8 of 10 important σ shake-up states. Second, a certain incidence of charge transfer (at least 0.1e) from the core-ionized atom is evident, occurring in 12 of the 33 important carbon 1s shake-up states and in 9 of the 20 important excited ionic states accompanying fluorine core ionization. Third, the expected relationship

between relaxation toward the core hole and satellite intensity is especially clear in some of the results.

The first of these trends is analogous to the charge transfer from the heteroatom to the ring calculated for the heterocyclics. The common feature is that in all the fluorinated hydrocarbons, the transition from high occupied to low-lying unoccupied π orbitals in the molecule involves transfer of on the average 0.3e from the fluorine(s) to the carbons; the similar transition in the heterocyclics involves a migration of about 0.4e from the heteroatom to the ring. In spite of the perturbation due to the core hole, one would expect a similar charge transfer in the shake-up transition, which is the calculated result.

Closely related to this phenomenon is the aspect of preferential stabilization of a molecular orbital predominantly composed of a certain atomic orbital when that atom is core-ionized. The effect of such stabilization has important consequences to shake-up energies, and is clearly evident in some of the data for the fluorinated hydrocarbons. When charge is transferred away from a fluorine atom in a shake-up transition, the final orbital is less fluorine-like than the initial orbital. For example, the 3π orbital in trans-1,2-difluoroethylene is delocalized over the molecule whereas the $4\pi^*$ orbital is of mostly carbon character. Thus, one would expect that the $3\pi \rightarrow 4\pi^*$ shake-up transition energy would be larger in the fluorine 1s spectrum that in

the carbon 1s spectrum because the 4π orbital is more stabilized by carbon core ionization than by a fluorine K-shell vacancy. Indeed, the observed and calculated low-energy shake-up state is of lower energy for carbon 1s ionization than it is in the case of fluorine. Similarly, the 8π orbital of hexafluorobenzene contains about 75% ring character whereas the $10\pi^*$ orbital is about 95% ring character. Therefore, the $8\pi \rightarrow 10\pi$ shake-up energy should be somewhat lower in the carbon core hole state than in the fluorine core hole state, which is both the observed and calculated result. This correlation is limited to cases in which an orbital assignment may be made to an experimental peak in an unambiguous way. For molecules such as vinyl fluoride, fluorobenzene, and 1,3,5-trifluorobenzene, a multiplicity of shake-up states resulting from core ionization of the inequivalent carbons overlap to produce a low-energy satellite, and such a correlation is impossible to identify.

The incidence of substantial charge transfer away from the core-ionized atom is less in the fluorinated hydrocarbons than in the heterocyclics. This phenomenon occurs in only about 40% of the important shake-up states of the former and in about 83% of those of the latter. To the extent that such charge transfer occurs in the fluorinated hydrocarbons, it may be rationalized on the same basis as it is for the heterocyclics; the weighted average of the

charge distributions of all the important ionic states must equal the Koopmans'-theorem distribution. Interestingly, charge transfer away from core-ionized fluorine in these molecules occurs twice as frequently in σ shake-up states as in π shake-up states. It would appear, then, that relaxation toward a K-shell vacancy on a fluorine is more substantial through σ orbitals than through the π orbitals in the ground ionic state. Correspondingly, there is more charge transfer away from that site through σ than π orbitals in the excited ionic states. Indeed, the CNDO/2 calculations show that the average difference between the Mulliken charge of the core-ionized fluorines in the ionic ground state and the molecular ground state is about 1.0e (no relaxation) in π orbitals and about 0.5e in the σ orbitals. It has been shown through UV photoelectron studies of fluorinated benzenes that increased fluorination stabilizes σ orbitals more than π orbitals, implying that the inductive effect is through the σ system (40). Thus, it would appear that the static inductive effect and the dynamic extra-atomic relaxation effect are both directed toward the fluorine primarily through the σ orbitals.

As mentioned in the theoretical section (Chapter II), the degree of electronic relaxation toward the core hole determines the deviation of the wave function for the ground state of the ion from the Koopmans'-theorem wave function, and hence the probability of populating excited states of

the ion. This expectation is clearly illustrated in the intensities of the $\pi \rightarrow \pi^*$ satellites for the fluorinated hydrocarbons. For each molecule, the intensity of the low-energy $\pi \rightarrow \pi^*$ shake-up state is substantially less for the fluorine 1s hole state(s) than for the carbon 1s hole states. On the basis of the relaxation argument, one would expect that there is less relaxation through the π orbitals for the K-shell vacancy on fluorine than for that on carbon. In fact, the π-orbital charge difference between the core-ionized atom in the ionic ground state and that in the molecule is on the average 1.0e for core-ionized fluorine and typically 0.6e for core-ionized carbon. This value is a measure of the relaxation toward the core hole in the ground state of the ion; small values indicate extensive relaxation. Relaxation through the π orbitals is clearly more extensive for carbon core ionization than it is for fluorine core ionization.

VII. CONCLUSION

Gas-phase measurements of satellite structure in molecules and atoms is superior to solid-phase measurements in that background effects due to inelastic electron scattering from the sample material can be minimized and subsequently eliminated from the data. The spectra of all the molecules studied in this work, with the exception of one (vinyl fluoride, fluorine 1s), show a clear distinction between low-energy $\pi \rightarrow \pi^*$ satellites and, when present, the high-energy structure due to single-electron σ-orbital shake-up, multi-electron effects, and shake-off.

Theoretical investigations using CNDO/2 wave functions provide, in most cases, qualitatively satisfactory agreement with experiment but in a small number of cases, a real sense of doubt as to the credibility of the approximation. In light of the relative simplicity and low expense involved in doing such calculations, CNDO/2 wave functions are probably worth the effort involved in generating them when studying states of systems that are likely to be adequately described by a simple valence basis set; the investigator must use his good judgment in discerning whether his system falls in this category.

Charge rearrangement accompanying photoionization of core levels is a highly complex process, yet certain trends

are observed. First, in many instances, charge is transferred away from the heteroatom or fluorine(s) to the carbons when shake-up states are populated, in keeping with the molecular orbital properties of the neutral molecule. Second, charge is sometimes transferred from the core-ionized atom during excited-ionic-state formation, in accord with the expectation of a Koopmans'-theorem-like distribution for the intensity-weighted average of the charge distributions of important ionic states. Third, if the molecular symmetry is modified during core ionization, other charge rearrangements that would not be expected from consideration of the neutral species can take place. Finally, the expected relationship between electronic relaxation toward the core hole and satellite intensity is observed; more relaxation results in greater shake-up intensity.

BIBLIOGRAPHY

1. T. Koopmans, Physica 1, 104 (1934).

2. M. O. Krause, T. A. Carlson, R. D. Dismukes, Phys. Rev., 170, 37 (1968).

3. L. I. Schiff, Quantum Mechanics, 3rd edition, McGraw-Hill Book Co., New York, 1968, p. 292.

4. T. A. Carlson, W. B. Dress, F. A. Grimm, and J. S. Haggerty, J. Electron Spectrosc. Relat. Phemon., 10, 147 (1977).

5. I. H. Hillier and J. Kendrick, Faraday Trans. II, 71, 1369 (1975).

6. D. T. Clark, D. B. Adams, A. Dilks, J. Peeling, and H. R. Thomas, J. Electron Spectrosc. Relat. Phenom., 8, 51 (1976).

7. R. L. Martin and D. A. Shirley, Phys. Rev. A, 13, 1475, (1976).

8. R. L. Martin, B. E. Mills, and D. A. Shirley, J. Chem. Phys., 64, 3690 (1976).

9. T. Ohta, T. Fujikawa, and H. Kuroda, Chem. Phys. Lett., 32, 369 (1975).

10. S. Pignataro, R. DiMarino, G. Distefano, and A. Mangini, Chem. Phys. Lett., 22, 352 (1973).

11. D. T. Clark and D. B. Adams, J. Electron Spectrosc. Relat. Phenom., 7, 401 (1975).

12. D. T. Clark and D. B. Adams, Theoret. Chim. Acta., 39, 321 (1975).

13. J. A. Pople and G. A. Segal, J. Chem. Phys., 44, 3289 (1966).

14. G. Herzberg, Molecular Spectra and Molecular Structure I, 2nd edition, D. Van Nostrand Co., Princeton, 1950, p. 55.

15. Ibid., p. 146.

16. E. U. Condon, Phys. Rev., 32, 858 (1928).

17. R. L. Martin and D. A. Shirley, J. Chem. Phys., 64, 3685 (1976).

18. E. Merzbacher, Quantum Mechanics, 2nd edition, John Wiley and Sons, New York, 1970, p. 470.

19. I. H. Hillier and V. R. Saunders, Mol. Phys., 22, 1025 (1971).

20. T. D. Thomas, J. S. Jen, S. A. Chambers, and K. D. Bomben, unpublished results.

21. M. Barber, J. A. Connor, M. F. Guest, M. B. Hall, I. H. Hillier, and W. N. E. Meredity, Farad. Diss. Chem. Soc., 54, 219 (1972).

22. M. Barber, J. A. Connor, and I. H. Hillier, Chem. Phys. Lett., 9, 570 (1971).

23. C. S. Fadley, Chem. Phys. Lett., 25, 225 (1974).

24. S. T. Manson, J. Electron Spectrosc. Relat. Phenom., 9, 21 (1976).

25. W. L. Jolly, in Electron Spectroscopy, edited by D. A. Shirley, North-Holland, Amsterdam, 1972, p. 629.

26. T. X. Carroll and T. D. Thomas, J. Electron Spectrosc. Relat. Phenom., 10, 215 (1977).

27. H. Basch, Chem. Phys., 10, 157 (1975).

28. U. Gelius, J. Electron Spectrosc. Relat. Phenom., 5, 1008 (1976).

29. C. C. J. Roothaan, Rev. Mod. Phys., 23, 69 (1951).

30. P. H. Citrin, R. W. Shaw, Jr., and T. D. Thomas, in Electron Spectroscopy, edited by D. A. Shirley, North-Holland, Amsterdam, 1972, p. 105.

31. K. Läuger, J. Phys. Chem. Solids, 32, 609 (1971).

32. S. R. Smith, Ph.D. Thesis, Oregon State University, 1977, p. 7.

33. T. D. Thomas and R. W. Shaw, Jr., J. Electron Spectrosc. Relat. Phenom., 5, 1081 (1974).

34. D. W. Davis, D. A. Shirley, and T. D. Thomas, J. Amer. Chem. Soc., 94, 6565 (1972).

35. T. X. Carroll, unpublished data.

36. Reference 32, p. 14.

37. Reference 32, p. 15.

38. U. Gelius, C. J. Allan, G. Johansson, H. Siegbahn, D. A. Allison, and K. Siegbahn, Physica Scripta, 3, 237 (1971).

39. T. Novakov and R. Prins, in Electron Spectroscopy, edited by D. A. Shirley, North-Holland, Amsterdam, 1972, p. 821.

40. W. C. Price, A. W. Potts, and T. A. Williams, Chem. Phys. Lett., 37, 17 (1976).

APPENDICES

APPENDIX A

X-ray Photoelectron Spectroscopy of Gaseous Nickel Carbonyl

Carbon monoxide is a small molecule that plays an important role in both molecular structure theory and surface chemistry. Being relatively simple, it may be investigated using the most advanced and sophisticated theoretical techniques. Because it is a starting material for the synthesis of a variety of more complex molecules, its surface chemistry has been extensively studied.

Nickel is frequently used as a substrate for studying adsorbtion of carbon monoxide on a metal surface. Nickel carbonyl represents an intermediate between free carbon monoxide and carbon monoxide bonded to a nickel surface. Studying nickel carbonyl in the gas phase allows accurate energy measurements of a compound involving nickel in its zero oxidation state without having to take into account extra-molecular interactions as must be done in solid-phase work.

Table I contains the results of the X-ray photoelectron spectra of gaseous nickel carbonyl measured by certain members of our research group. Included are ionization potentials for the nickel 2p, carbon 1s, and oxygen 1s orbitals and satellite energies and intensities for the latter two.

Table I. Core ionization potentials and satellite structure in gaseous nickel carbonyl, carbon monoxide, and nickel.

	$Ni(CO)_4$			CO			Ni[b]
	I(%)	ΔE(eV)	E_{ABS}(eV)	I(%)	ΔE(eV)	E_{ABS}(eV)	E_{ABS}(eV)
C(1s)	100	0	293.79(5)[e]	100	0[c]	296.24(3)[a,e]	
	46	5.83(5)		3.1	8.3		
				0.3	11.4		
				5.6	14.9		
				2.6	17.8		
				2.0	19.1		
				1.4	20.0		
				0.6	20.8		
				3.9	23.2		
				4	26.1		
				2	28.8		
O(1s)	100	0	540.09(4)	100	0[d]	542.57(3)[a]	
	34	5.93(4)		19	15		
$Ni(2p_{1/2})$			878.17(8)				886
$Ni(2p_{3/2})$			861.06(4)				870

a. Reference 1.
b. Reference 2.
c. Reference 8.
d. Reference 9.
e. Figures in parentheses give the uncertainty in the last digit.

For comparison, data have been included for carbon monoxide in the gas-phase (1) and for free-atom nickel (2).

If one first inspects the core ionization potentials, it is clear that all values are lower in $Ni(CO)_4$ than in the free ligand and nickel atom. This result is inconsistent with expectations based on changes in initial-state charge distribution. If such initial-state effects dominated, one would expect some ionization potentials in the molecule to go up relative to those of the free atom and ligands and others to go down, since electrons removed from one atom during bond formation must be deposited on another. An alternative explanation is extra-atomic relaxation. If in the molecular environment, each atom is surrounded by polarizable material, then core ionization of the atom would lead to a final state that is stabilized by charge transfer and polarization toward the hole, lowering the binding energy relative to what it is in the free atom. According to the arguments presented in Chapter II of the text, extensive relaxation should result in intense satellite structure. Indeed, the carbon and oxygen 1s spectra show remarkably intense low-energy satellites, whose energies and intensities are in good agreement with those reported by Barber, Connor and Hillier for solid $Ni(CO)_4$ (3). However, the nickel 2p spectrum shows none! CNDO/2 calculations (4) done for $Ni(CO)_4$ and its equivalent-cores species, $Cu(CO)_4^+$, indicate extensive relaxation toward the nickel core hole. The

Mulliken charge of the nickel in the molecule is -1.4e and that in the ionic ground is -1.3e, indicating that nearly 1e has relaxed from the ligands to the metal hole. As one would expect, the calculated shake-up intensity for the low-lying $5t_2 \rightarrow 6t_2$ transition is large, approximately 20%. However, no satellite intensity of any kind is present in the experimental spectrum, casting serious doubt on the validity of the calculation and the reality of the predicted extra-atomic relaxation toward the core-ionized nickel. If the relationship between satellite intensity and relaxation developed in this work is correct, it may be concluded that extra-atomic relaxation toward the nickel L-shell vacancy is rather insignificant.

But why is there such a large binding energy shift in going from free-atom nickel to $Ni(CO)_4$ with the nickel in its zero oxidation state? It should be noted that a similar shift is observed when free-atom nickel is condensed into a solid (5). In this case, there is a change in electron configuration from $2d^8 4s^2$ to $3d^9 4s^1$. Since 3d electrons are, on the average, closer to the core than are the 4s electrons, there is a stronger repulsive potential for the core electrons in condensed nickel and hence a lower ionization potential (6). Calculations by Hillier and Saunders (7) indicate that the electron configuration in nickel carbonyl is $d^{9.3}$; a similar effect is, therefore, presumably important in this case as well. A calculation involving the equivalent-cores

approximation shows that there would be about a 10 eV decrease in core ionization potential when the configuration changes from $3d^8 4s^2$ to $3d^{10} 4s^0$, even though there is no change in oxidation number.

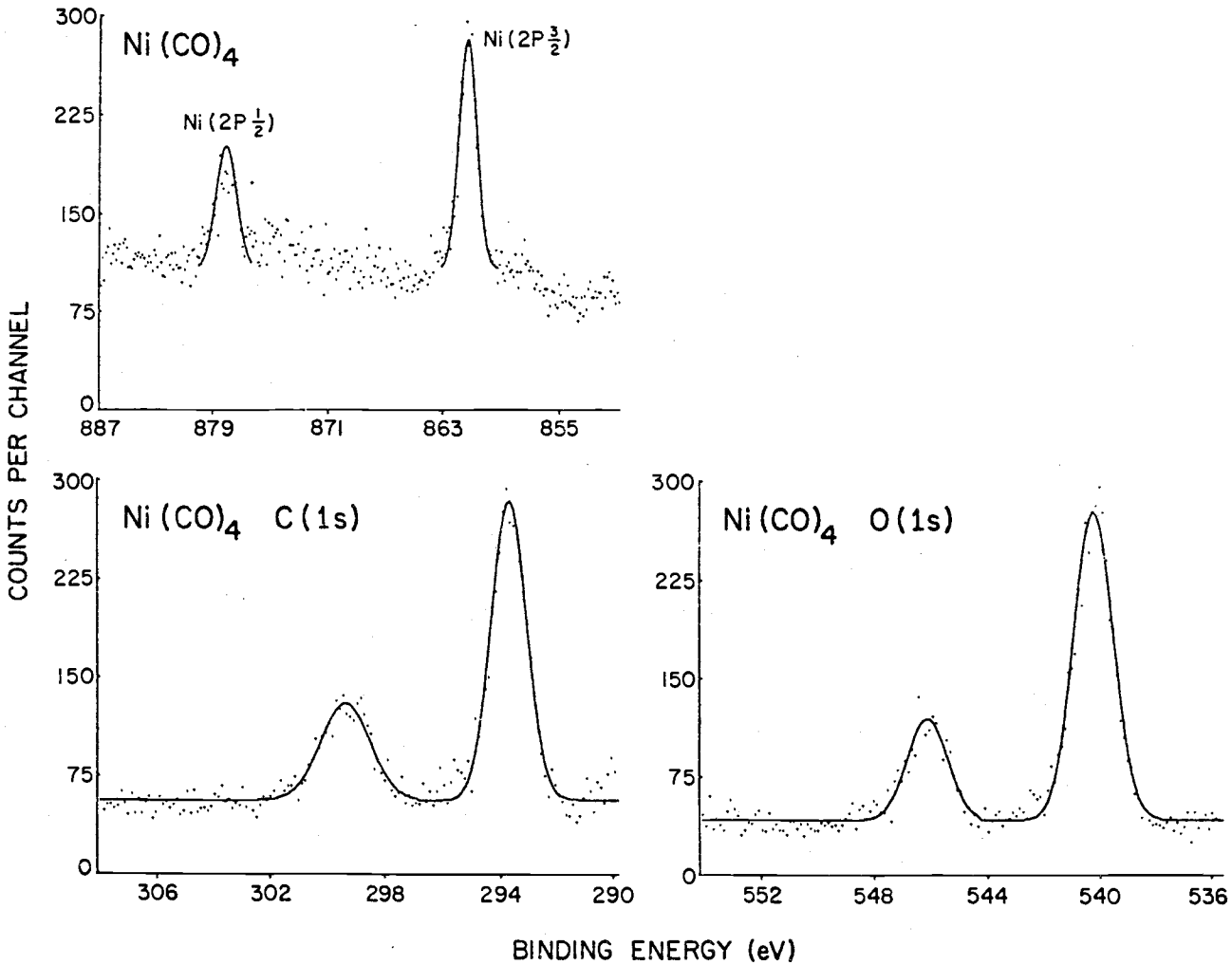

Figure 1. X-ray (AlKα) photoelectron spectra of gaseous nickel carbonyl. Solid lines show least-squares fits to the data.

REFERENCES

1. S. R. Smith and T. D. Thomas, J. Electron Spectrosc. Spectrosc. Relat. Phenom., 8, 45 (1976).

2. D. A. Shirley, R. L. Martin, S. P. Kowalczyk, F. R. McFeely, and L. Ley, Lawrence Berkeley Laboratory Report, LBL 4065 (1975).

3. M. Barber, J. A. Connor, and I. H. Hillier, Chem. Phys. Lett., 9, 570 (1971).

4. Peter Sherwood, University of Newcastle, private communication.

5. L. Ley, S. P. Kowalczyk, F. R. McFeely, R. A. Pollak, and D. A. Shirley, Phys. Rev. B, 8, 2392 (1973).

6. R. E. Watson, M. L. Perlman, and J. F. Herbst, Phys. Rev. B, 13, 2358 (1976).

7. I. H. Hillier and V. R. Saunders, Mol. Phys., 22, 1025 (1971).

8. U. Gelius, J. Electron Spectrosc. Relat. Phenom., 5, 1003 (1974).

9. R. W. Shaw, Jr., and T. D. Thomas, Chem. Phys. Lett., 14, 121 (1972).

APPENDIX B

Changes in Mulliken Charge (in units of 0.01e) in Going from the Ground Ionic State to the Indicated Shake-up State for the Molecules Investigated in this Work (derived separately for σ and π orbitals)

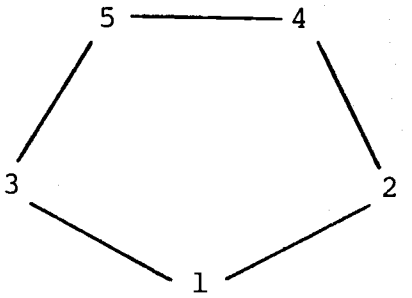

Molecule and State	1	2	3	4	5
Furan (Cls)	O	N	C	C	C
3a" → 4a"	8	-19	4	41	-33
2a" → 4a"	-44	7	29	16	- 9
Furan C(ls)	O	C	C	N	C
2a" → 4a"	-36	59	3	-19	- 7
Firan O(ls)	F	C	C	C	C
$2b_1 \rightarrow 3b_1$	-22	20	20	-10	-10
Pyrrole C(ls)	N	N	C	C	C
3a" → 4a"	-16	11	24	20	-40
2a" → 4a"	- 6	-23	7	23	- 3
Pyrrole C(ls)	N	C	C	N	C
2a" → 4a"	-24	55	- 4	-26	- 2
Pyrrole N(ls)	O	C	C	C	C
$2b_1 \rightarrow 3b_1$	-31	26	26	-10	-10
Thiophen C(ls)	S	N	C	C	C
2a" → 4a"	3	-23	2	34	-16
Thiophen C(ls)	S	C	C	N	C
2a" → 4a"	-12	52	-23	-10	- 8
2a" → 5a"	-23	- 5	12	-23	38
Thiophen S(2p)	CL	C	C	C	C
$2b_1 \rightarrow 3b_1$	-68	29	29	6	6

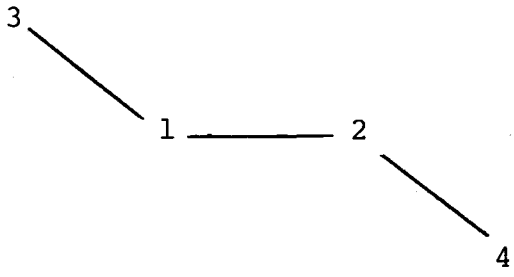

Molecule and State	1	2	3	4
Ethylene C(1s)	N	C		
$\pi \rightarrow \pi^*$	-40	40		
Vinyl Fluoride C(1s)	N	C	F	
$2\pi \rightarrow 3\pi^*$	-12	44	-32	
$1\pi \rightarrow 3\pi^*$	4	62	-66	
Vinyl Fluoride C(1s)	C	N	F	
$2\pi \rightarrow 3\pi^*$	59	-34	-25	
Vinyl Fluoride F(1s)	C	C	Ne	
$2\pi \rightarrow 3\pi^*$	-16	18	- 2	
$1\pi \rightarrow 3\pi^*$	38	59	-97	
Trans-1-2-Difluoroethylene C(1s)	C	N	F	F
$3\pi \rightarrow 4\pi^*$	56	-20	-13	-23
$1\pi \rightarrow 4\pi^*$	53	- 1	-15	-37
Trans-1-2-Difluoroethylene F(1s)	C	C	Ne	F
$3\pi \rightarrow 4\pi^*$	-16	41	- 2	-23
$1\pi \rightarrow 4\pi^*$	33	60	-96	3

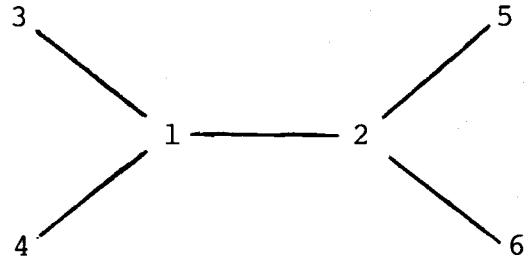

Molecule and State	1	2	3	4	5	6
Ethylene C(1s)	N	C	H	H	H	H
$5\sigma \rightarrow 9\sigma^*$	- 5	12	- 5	- 5	1	1
$4\sigma \rightarrow 8\sigma^*$	-37	3	- 2	- 2	19	19
$3\sigma \rightarrow 7\sigma^*$	-12	-19	14	14	2	2
$2\sigma \rightarrow 6\sigma^*$	6	-29	22	22	-10	-10
$1\sigma \rightarrow 6\sigma^*$	-21	-21	21	21	0	0
Vinyl Fluoride C(1s)	N	C	F	H	H	H
$7\sigma \rightarrow 11\sigma^*$	6	8	-10	- 6	- 4	6
$5\sigma \rightarrow 10\sigma^*$	-15	10	-33	2	21	15
$4\sigma \rightarrow 9\sigma^*$	0	-13	-13	13	8	5
$3\sigma \rightarrow 8\sigma^*$	3	-15	0	23	-10	- 2
Vinyl Fluoride C(1s)	C	N	F	H	H	H
$3\sigma \rightarrow 8\sigma^*$	-21	11	-12	-12	12	22
$2\sigma \rightarrow 8\sigma^*$	- 6	-23	- 9	8	14	16
Vinyl Fluoride F(1s)	C	C	Ne	H	H	H
$7\sigma \rightarrow 8\sigma^*$	48	-31	6	-12	-17	6
$6\sigma \rightarrow 8\sigma^*$	51	-44	3	2	5	-16
$5\sigma \rightarrow 8\sigma^*$	42	-24	- 2	-13	-10	9
$4\sigma \rightarrow 8\sigma^*$	62	- 3	-74	0	5	9
$3\sigma \rightarrow 8\sigma^*$	56	- 3	-68	2	3	9
$1\sigma \rightarrow 8\sigma^*$	63	2	-83	3	5	10

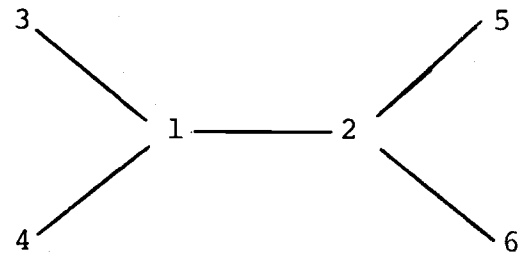

Molecule and State	1	2	3	4	5	6
Trans-1,2,-difluoro-ethylene C(1s)	C	N	F	H	H	F
$9\sigma \rightarrow 12\sigma^*$	17	- 2	-14	6	11	-17
$6\sigma \rightarrow 11\sigma^*$	3	6	-31	20	4	- 2
$4\sigma \rightarrow 10\sigma^*$	-13	5	- 6	- 9	20	3
$3\sigma \rightarrow 10\sigma^*$	- 3	- 6	- 8	7	27	-17
Trans-1,2,-difluoro-ethylene F(1s)	C	C	Ne	H	H	F
$8\sigma \rightarrow 10\sigma^*$	64	-14	6	- 5	2	-53
$4\sigma \rightarrow 10\sigma^*$	62	1	-71	- 2	3	8
$5\sigma \rightarrow 10\sigma^*$	59	- 3	-59	- 1	4	0
$1\sigma \rightarrow 10\sigma^*$	65	3	-82	0	4	9

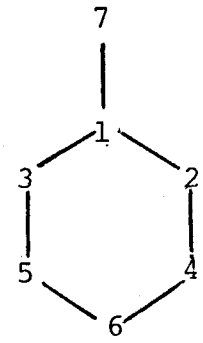

Molecule and State	1	2	3	4	5	6	7
Benzene C(1s)	N	C	C	C	C	C	
$3\pi \rightarrow 4\pi^*$	25	- 5	- 5	-23	-23	30	
$1\pi \rightarrow 4\pi^*$	- 4	4	4	-12	-12	19	
Fluorobenzene C(1s)	N	C	C	C	C	C	F
$4\pi \rightarrow 6\pi^*$	-12	19	19	- 9	- 9	4	-11
Fluorobenzene C(1s)	C	N	C	C	C	C	F
$3\pi \rightarrow 5\pi^*$	19	-19	-16	21	3	- 9	1
Fluorobenzene C(1s)	C	C	C	N	C	C	F
$3\pi \rightarrow 5\pi^*$	- 1	14	2	- 5	-27	19	- 3
Fluorobenzene C(1s)	C	C	C	C	C	N	F
$4\pi \rightarrow 5\pi^*$	24	-21	-21	6	6	11	- 6
$3\pi \rightarrow 5\pi^*$	20	-18	-18	12	12	3	-11
Fluorobenzene F(1s)	C	C	C	C	C	C	Ne
$3\pi \rightarrow 5\pi^*$	- 1	12	12	- 9	- 9	- 4	- 1

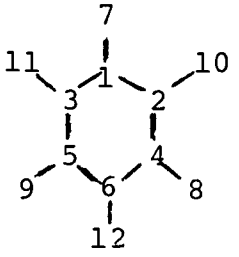

Molecule & State	1	2	3	4	5	6	7	8	9	10	11	12
1,3,5-Trifluoro-benzene C(1s)	N	C	C	C	C	C	F	F	F			
$5\pi \rightarrow 7\pi^*$	4	20	20	- 7	- 7	- 6	- 5	- 9	- 9			
$4\pi \rightarrow 7\pi^*$	14	12	12	1	1	25	-23	-21	-21			
1,3,5-Trifluoro-benzene C(1s)	C	N	C	C	C	C	F	F	F			
$5\pi \rightarrow 7\pi^*$	21	-13	-15	21	17	-15	2	2	-20			
$4\pi \rightarrow 7\pi^*$	19	- 7	- 2	19	31	- 2	-24	-24	-10			
1,3,5-Trifluoro-benzene F(1s)	C	C	C	C	C	C	Ne	F	F			
$5\pi \rightarrow 7\pi^*$	14	13	13	- 5	- 5	-14	0	- 8	- 8			
$4\pi \rightarrow 7\pi^*$	13	6	6	4	4	25	- 1	-28	-28			
$1\pi \rightarrow 7\pi^*$	31	14	14	4	4	25	-94	0	0			
Hexafluoro-benzene C(1s)	N	C	C	C	C	C	F	F	F	F	F	F
$7\pi \rightarrow 10\pi^*$	- 2	21	21	-10	-10	10	- 4	- 8	- 8	2	2	-12
Hexafluoro-benzene F(1s)	C	C	C	C	C	C	Ne	F	F	F	F	F
$8\pi \rightarrow 10\pi^*$	6	16	16	- 8	- 8	6	0	- 7	- 7	1	1	-14
$7\pi \rightarrow 10\pi^*$	4	12	12	2	2	28	- 1	- 8	- 8	-20	-20	- 2

APPENDIX C

FORTRAN IV Programs Generated for Performing Theoretical Calculations and Data Analyses

```
T TT-DT1 CORRST SRC

C       THIS PROGRAM CALCULATES THE PROBABILITY THAT VARIOUS
C       SHAKE-UP STATES WILL RESULT FROM CORE IONIZATION
C       OF AN ATOM IN A MOLECULE BY DIPOLE INTERACTION WITH A
C       RADIATION FIELD OF SOFT X-RAYS USING CNDO/2 WAVEFUNCTIONS.
C       IT DOES SO BY CALCULATING THE SCALAR PRODUCT OF DETERMINANTAL
C       WAVEFUNCTIONS FOR THE INITIAL MOLECULE AND VARIOUS CORRELATION
C       STATES PRODUCED BY ONE ELECTRON EXCITATIONS FROM EACH OCCUPIED
C       ORBITAL IN THE EQUIVALENT CORES ION TO ALL POSSIBLE UNOCCUPIED
C       ORBITALS.
C       DEFINITION OF PARAMETERS:
C          N=THE NUMBER OF BASIS SET FUNCTIONS PER ORBITAL WAVEFUNCTION.
C          NA=THE NUMBER OF INITIAL STATE MOLECULAR ORBITALS.
C          NB=THE NUMBER OF FINAL STATE MOLECULAR ORBITALS.
C          A=THE MATRIX OF INITIAL STATE WAVEFUNCTIONS.
C          B=THE MATRIX OF FINAL STATE WAVEFUNCTIONS.
C          S=THE MASTER MATRIX WHOSE ELEMENTS ARE SCALAR PRODUCTS OF
C          ORBITALS: ONE FROM THE MOLECULE AND ONE FROM THE EQUIVALENT
C          CORES ION, TAKEN OVER ALL POSSIBLE PAIRS.
C          Q=SUBMATRICES WHOSE DETERMINANT SQUARED GIVES PROBABILITIES
C          FOR THE PRODUCTION OF THE VARIOUS CORRELATION STATES.
C
C       MAIN PROGRAM CORRST
        COMMON NA,NB,N,A(10,15),B(15,15),FILLER(776)
1       PAUSE
        CALL INPUT
        CALL MASMAT
        CALL SUBMGS
        CALL SUBMCS
        CALL OUTPUT
        GO TO 1
        END

PIP V13A

>T TT-DT1 INPUT SRC

        SUBROUTINE INPUT
        COMMON NA,NB,N,A(10,15),B(15,15),FILLER(776)
        WRITE(4,10)
10      FORMAT(6H TITLE)
        WRITE(4,15)
15      FORMAT(38H NUMBER OF BASIS FUNCTIONS PER ORBITAL)
        READ(4,20) N
20      FORMAT(I2)
        WRITE(4,35)
35      FORMAT(43H NUMBER OF INITIAL STATE MOLECULAR ORBITALS)
        READ(4,20) NA
        WRITE(4,40)
40      FORMAT(41H NUMBER OF FINAL STATE MOLECULAR ORBITALS)
        READ(4,20) NB
        WRITE(4,51)
51      FORMAT(40H INSERT TAPE OF MOLECULAR EIGENFUNCTIONS)
        PAUSE 1
53      DO 54 I=1,NA
        READ(2,35) (A(I,K), K=1,N)
54      CONTINUE
```

```
      WRITE(4,81)
81    FORMAT(47H INSERT TAPE OF EQUIVALENT CORES EIGENFUNCTIONS)
      PAUSE 2
83    DO 84 I=1,NB
      READ(2,85) (B(I,K), K=1,N)
84    CONTINUE
85    FORMAT(10F7.4)
      RETURN
      END

PIP V13A

>T TT-DT1 MASMAT SRC

C     THIS PROGRAM CALCULATES THE MASTER MATRIX S.
      SUBROUTINE MASMAT
      COMMON NA,NB,N,A(10,15),B(15,15),FILLER(776)
      COMMON/C10/NA2,NB2,S(20,30)
      NA2=NA*2
      NB2=NB*2
      DO 20 I=1,NA
      DO 15 J=1,NB
      IM=I-1
      JM=J-1
      L=2*IM+1
      K=2*JM+1
      P=0.
      DO 10 KN=1,N
      P=P+A(I,KN)*B(J,KN)
10    CONTINUE
      S(L,K)=P
      L1=L+1
      K1=K+1
      S(L1,K1)=P
15    CONTINUE
20    CONTINUE
      DO 30 I=1,NA2,2
      DO 25 J=2,NB2,2
      S(I,J)=0.
      I1=1+I
      J1=J-1
      S(I1,J1)=0.
25    CONTINUE
30    CONTINUE
      RETURN
      END

PIP V13A

>T TT-DT1 SUBMGS SRC

C     THIS PROGRAM CONSTRUCTS THE SUBMATRIX FOR THE GROUND STATE
C     OF THE ION FROM THE MASTER MATRIX AND CALCULATES ITS
C     DETERMINANT.
      SUBROUTINE SUBMGS
      DOUBLE PRECISION Q
      COMMON NA,NB,N,Q(20,20),Y(10,15),X
```

```
      COMMON/C10/NA2,NB2,S(20,30)
      DO 15 I=1,NA2
      DO 10 J=1,NA2
      Q(I,J)=S(I,J)
10    CONTINUE
15    CONTINUE
      X=DETERM(NA2)
      X=X**2
      RETURN
      END
```

```
PIP V13A

>T TT-DT1 SUBMCS SRC
```

```
C       THIS PROGRAM CONSTRUCTS SUBMATRICES FOR THE VARIOUS CORRELATION
C       STATES FROM THE MASTER MATRIX AND EVALUATES THEIR DETERMINANTS.
        SUBROUTINE SUBMCS
        DOUBLE PRECISION Q
        COMMON NA,NB,N,Q(20,20),Y(10,15),X
        COMMON/C10/NA2,NB2,S(20,30)
        NA22=NA2+2
        DO 20 K=2,NA2,2
        DO 15 L=NA22,NB2,2
        DO 10 I=1,NA2
        DO 5 J=1,NA2
        IF (J .EQ. K) Q(I,J)=S(I,L)
        IF (J .NE. K) Q(I,J)=S(I,J)
5       CONTINUE
10      CONTINUE
        K2=K/2
        L2=L/2
        Y(K2,L2)=DETERM(NA2)
        Y(K2,L2)=(Y(K2,L2)**2)*2.
15      CONTINUE
20      CONTINUE
        RETURN
        END
```

```
PIP V13A

>T TT-DT1 DETERM SRC
```

```
C       THIS PROGRAM CALCULATES THE DETERMINANT OF A SQUARE MATRIX.
        FUNCTION DETERM(NORDER)
        DOUBLE PRECISION Q,SAVE
        COMMON NA,NB,N,Q(20,20),Y(10,15),X
10      DETERM=1.
11      DO 50 K=1,NORDER
C       INTERCHANGE COLUMNS IF DIAGONAL ELEMENT IS ZERO
        IF (Q(K,K)) 41,21,41
21      DO 23 J=K,NORDER
        IF (Q(K,J)) 31,23,31
23      CONTINUE
        DETERM=0.
        GO TO 60
31      DO 34 I=K,NORDER
```

```
      SAVE=Q(I,J)
      Q(I,J)=Q(I,K)
34    Q(I,K)=SAVE
      DETERM=-DETERM
C     SUBTRACT ROW K FROM LOWER ROWS TO GET DIAGONAL MATRIX
41    DETERM=DETERM*Q(K,K)
      IF (K-NORDER) 43,50,50
43    K1=K+1
      DO 46 I=K1,NORDER
      DO 46 J=K1,NORDER
46    Q(I,J)=Q(I,J)-Q(I,K)*Q(K,J)/Q(K,K)
50    CONTINUE
60    RETURN
      END

PIP V13A

>T TT-DT1 OUTPUT SRC

      SUBROUTINE OUTPUT
      DOUBLE PRECISION Q
      COMMON NA,NB,N,Q(20,20),Y(10,15),X
      WRITE(4,10) X
10    FORMAT(42H INTENSITY TO THE GROUND STATE OF THE ION=,F8.6)
      WRITE(4,20)
20    FORMAT(55H INITIAL ORBITAL   FINAL ORBITAL   SHAKE-UP PROBABILITY)
      NA1=NA+1
      DO 30 K=1,NA
      DO 25 L=NA1,NB
      WRITE(4,35) K,L,Y(K,L)
25    CONTINUE
30    CONTINUE
35    FORMAT(7H         ,I2,14H                ,I2,14H                ,F8.6
     1)
      RETURN
      END

PIP V13A

>
```

```
T TT-DTI ENCOR2 SRC

C       THIS PROGRAM CALCULATES THE ENERGY CORRECTIONS TO THE CALCULATED
C       CNDO TRANSITION ENERGIES FOR "HOMO" TO "LUMO" TYPE
C       TRANSITIONS WHICH ARE IN ERROR BY THE DIFFERENCE BETWEEN COULOMB
C       AND EXCHANGE INTEGRALS FOR THE TWO ORBITALS.
C       DEFINITION OF PARAMETERS:
C          IA=ATOM IDENTIFICATION NUMBER FOR EACH ORBITAL
C          A=EQUIVALENT CORES EIGENFUNCTIONS
C          C=COULOMB INTEGRAL MATRIX
C          N=THE NUMBER OF BASIS SET FUNCTIONS USED
        COMMON IA(15), FILEN(2), C(15,15), A(15,15)
        PAUSE
        WRITE(4,5)
5       FORMAT(6H TITLE)
        WRITE(4,35)
        READ(4,15) N
15      FORMAT(I2)
        WRITE(4,11)
11      FORMAT(37H DIMENSION OF COULOMB INTEGRAL MATRIX)
        READ(4,15) M
        WRITE(4,10)
10      FORMAT(36H INSERT COULOMB INTEGRAL MATRIX TAPE)
        PAUSE
21      FORMAT(2A5)
        DO 25 I=1,M
        READ(5,30) (C(I,J), J=1,M)
25      CONTINUE
        WRITE(4,26)
26      FORMAT(34H /COULOMB INTEGRAL MATRIX ELEMENTS)
30      FORMAT(10F7.4)
35      FORMAT(42H NUMBER OF BASIS SET FUNCTIONS PER ORBITAL)
44      WRITE(4,45)
45      FORMAT(49H NAME OF FILE FOR EQUIVALENT CORES EIGENFUNCTIONS)
        READ(4,21) FILEN(1),FILEN(2)
        CALL SEEK(2,FILEN)
        DO 56 I=1,N
        READ(2,30) (A(I,J), J=1,N)
56      CONTINUE
        CALL CLOSE(2)
59      WRITE(4,60)
60      FORMAT(31H ORBITAL EXPANSION COEFFICIENTS)
        WRITE(4,75)
75      FORMAT(51H ATOM IDENTIFICATION NUMBER FOR EACH ORBITAL (23I3))
        WRITE(4,80)
80      FORMAT(70H  .. .. .. .. .. .. .. .. .. .. .. .. .. .. .. .. .. ..
       1 .. .. .. .. ..)
        READ(4,90) (IA(I), I=1,N)
90      FORMAT(23I3)
        WRITE(4,105)
C       CALCULATION OF THE ENERGY CORRECTION
        DO 101 I3=1,N
        DO 101 J3=1,N
        IF (J3 .LE. I3) GO TO 101
91      SUMJ=0.0
        SUMK=0.0
        DO 100 I=1,N
        DO 100 J=1,N
        DO 100 K=1,N
        DO 100 L=1,N
```

```
      IF (I .NE. J) GO TO 95
      IF (K .NE. L) GO TO 95
      I1=IA(I)
      K1=IA(K)
      CINT=C(I1,K1)
      SUMJ=A(I3,I)*A(I3,J)*A(J3,K)*A(J3,L)*CINT+SUMJ
95    IF (I .NE. K) GO TO 100
      IF (J .NE. L) GO TO 100
      I2=IA(I)
      J2=IA(J)
      CINT=C(I2,J2)
      SUMK=A(I3,I)*A(I3,J)*A(J3,K)*A(J3,L)*CINT+SUMK
100   CONTINUE
      SUMJ=SUMJ*27.21
      SUMK=SUMK*27.21
      EC=SUMJ-SUMK*2.
      WRITE(4,106) I3,J3,EC
101   CONTINUE
105   FORMAT(57H INITIAL ORBITAL   FINAL OBEITAL   ENERGY CORRECTION (EV
     1))
106   FORMAT(7H        ,I2,14H              ,I2,15H                  ,F5.2)
      END

PIP V13A

>
```

```
 T TT-DT1 MULPOP SRC

C      THIS PROGRAM CALCULATES MULLIKEN POPULATIONS FROM CNDO/2 MOLECULAR
C      ORBITAL WAVE FUNCTIONS FOR GROUND STATES AND ONE-ELECTRON
C      EXCITED STATES.
       COMMON A(15,15),B(10,15)
1      PAUSE
C
C      INPUT OF WAVE FUNCTIONS
C
       WRITE(4,10)
10     FORMAT(6H TITLE)
       WRITE(4,15)
15     FORMAT(38H NUMBER OF BASIS FUNCTIONS PER ORBITAL)
       READ(4,20) N
20     FORMAT(I2)
       WRITE(4,25)
25     FORMAT(28H NUMBER OF OCCUPIED ORBITALS)
       READ(4,20) NA
       WRITE(4,26)
26     FORMAT(25H TOTAL NUMBER OF ORBITALS)
       READ(4,20) NB
       WRITE(4,30)
30     FORMAT(30H INSERT TAPE OF EIGENFUNCTIONS)
       PAUSE
       DO 40 I=1,NB
       READ(5,45) (A(I,J), J=1,N)
40     CONTINUE
45     FORMAT(10F7.4)
C
C      CALCULATION OF THE GROUND STATE POPULATION
C
       WRITE(4,46)
46     FORMAT(13H GROUND STATE)
       WRITE(4,47)
47     FORMAT(44H ATOMIC ORBITAL NUMBER    MULLIKEN POPULATION)
       DO 55 J=1,N
       S=0.
       DO 50 I=1,NA
       S=S+A(I,J)**2
50     CONTINUE
       S=S*2.
       WRITE(4,60) J,S
55     CONTINUE
60     FORMAT(5H      ,I2,26H                              ,F6.3)
       WRITE(4,65)
65     FORMAT(60H FOR POPULATIONS OF EXCITED STATES, TYPE 1, OTHERWISE TY
     1PE 2)
       READ(4,70) M1
70     FORMAT(I1)
       GO TO (75,1), M1
C
C      CALCULATION OF EXCITED STATE POPULATIONS
C
75     NA1=NA+1
       WRITE(4,77)
77     FORMAT(15H EXCITED STATES)
       WRITE(4,78)
78     FORMAT(55H FROM M.O.       TO M.O.       ATOM   MULLIKEN POPULATION)
```

```
      DO 95 K=1,NA
      DO 90 L=NA1,NB
      DO 85 J=1,N
      S=0.
      DO 80 I=1,NA
      IF(I .NE. K) B(I,J)=(A(I,J)**2)*2.
      IF(I .EQ. K) B(I,J)=A(I,J)**2+A(L,J)**2
      S=S+B(I,J)
80    CONTINUE
      WRITE(4,100) K,L,J,S
85    CONTINUE
90    CONTINUE
95    CONTINUE
100   FORMAT(5H      ,I2,11H            ,I2,10H           ,I2,11H
     1   ,F6.3)
      END

PIP V13A

>
```

T TT-DT1 ELCOR3 SRC

```
C       THIS PROGRAM CALCULATES THE CORRECTED SHAKE-UP AND NORMALIZED
C       ENERGY LOSS SPECTRA FROM DAN1 DATA OF UP TO 256 CHANNELS.
C       AN OPTIONAL SMOOTHING ROUTINE IS INCLUDED.
        COMMON ISU(261), IEL(261), ISUCOR(261), IELNOR(261), TITL1(15),
       1TITL2(15),TITL3(15),TITL4(15),ISCSMT(261),IC(20)
        PAUSE
        WRITE(4,4)
4       FORMAT(26H INSERT SHAKE-UP DATA TAPE)
        PAUSE
        WRITE(4,5)
5       FORMAT(47H NUMBER OF DATA CONTAINING CHANNELS, FORMAT(I3))
        READ(4,10)N
10      FORMAT(I3)
        READ(5,15) (TITL1(I), I=1,15)
15      FORMAT(14A5,A2)
        WRITE(4,20) (TITL1(I), I=1,15)
20      FORMAT(1HO,14A5,A2)
        M=N+5
        READ(5,25) (ISU(J), J=1,M)
25      FORMAT(I6)
        WRITE(4,30)
30      FORMAT(29H INSERT ENERGY LOSS DATA TAPE)
        PAUSE
        READ(5,15) (TITL2(K), K=1,15)
        WRITE(4,20) (TITL2(K), K=1,15)
        READ(5,25) (IEL(L), L=1,M)
        WRITE(4,45)
45      FORMAT(51H BACKROUND IN THE ENERGY LOSS SPECTRUM FORMAT(F6.2))
        READ(4,40)BEL
40      FORMAT(F6.2)
        WRITE(4,50)
50      FORMAT(19H ALPHA FORMAT(F6.4))
        READ(4,55)A
55      FORMAT(F6.4)
        WRITE(4,56)
56      FORMAT(41H STARTING CHANNEL FOR CORRECTED DATA (I3))
        READ(4,57) N1
57      FORMAT(I3)
        N1=N1+5
C       CALCULATION OF THE CORRECTED SHAKE-UP SPECTRUM
        DO 60 I=1,M
        S=ISUCOR(I)
        P=ISU(I)
        Q=IEL(I)
        R=IELNOR(I)
        R=A*(Q-BEL)
        S=P-R
        IF (I .LT. N1) ISUCOR(I)=P
        IF (I .GE. N1) ISUCOR(I)=S
        IELNOR(I)=R
        IF (IELNOR(I) .LT. 0) IELNOR(I)=-IELNOR(I)
60      CONTINUE
        WRITE(4,65)
65      FORMAT(23H TO SMOOTH DATA=1, NO=2)
        READ(4,10) I
        GO TO (70,100), I
70      WRITE(4,71)
71      FORMAT(39H M     (NUMBER OF POINTS PER FIT=2*M+1) )
```

```
      READ(4,10) MA
      NA=2*MA+1
      DO 72 J=1,NA
      I=J-MA-1
72    IC(J)=3*(3*MA*MA+3*MA-1-5*I*I)
      IN=(2*MA-1)*(2*MA+1)*(2*MA+3)
      MN=M-MA
      MM=MA+6
      DO 75 I=MM,MN
      ISUM=0
      SUM=0.
      DO 73 J=1,NA
      K=I+J-MA-1
      C=IC(J)
      Y=ISUCOR(K)
      AIN=IN
73    SUM=SUM+C*Y/AIN
75    ISCSMT(I)=SUM/1.
      DO 80 I=MM,MN
80    ISUCOR(I)=ISCSMT(I)
100   WRITE(4,101)
101   FORMAT(34H TITLE FOR CORRECTED SHAKE-UP TAPE)
      READ(4,102) (TITL3(I), I=1,15)
102   FORMAT(14A5,A2)
      WRITE(6,103) (TITL3(I), I=1,15)
103   FORMAT(1X,14A5,A2)
      WRITE(6,104) (ISUCOR(J), J=1,M)
104   FORMAT(1X,I6)
110   WRITE(4,111)
111   FORMAT(38H TITLE FOR NORMALIZED ENERGY LOSS TAPE)
      READ(4,102) (TITL4(I), I=1,15)
      WRITE(6,103) (TITL4(J), J=1,15)
      WRITE(6,104) (IELNOR(K), K=N1,M)
      GO TO 4
      END

PIP V13A

>
```

```
T TT-ITI GAUSSN SR(

C     THIS PROGRAM GENERATES TWO GAUSSIAN FUNCTIONS ON DATA TAPE
      COMMON IX(500),TITLE(15)
      WRITE(4,5)
5     FORMAT(19H NUMBER OF CHANNELS)
      READ(4,10) NCHN
10    FORMAT(I3)
      WRITE(4,15)
15    FORMAT(23H POSITION OF FIRST PEAK)
      READ(4,20) P1
20    FORMAT(F6.2)
      WRITE(4,25)
25    FORMAT(24H POSITION OF SECOND PEAK)
      READ(4,20) P2
      WRITE(4,30)
30    FORMAT(20H SIGMA OF FIRST PEAK)
      READ(4,35) S1
35    FORMAT(F4.2)
      WRITE(4,40)
40    FORMAT(21H SIGMA OF SECOND PEAK)
      READ(4,35) S2
      WRITE(4,45)
45    FORMAT(19H AREA OF FIRST PEAK)
      READ(4,48) AREA1
      WRITE(4,46)
46    FORMAT(20H AREA OF SECOND PEAK)
      READ(4,48) AREA2
48    FORMAT(F7.2)
      WRITE(4,50)
50    FORMAT(20H BACKGROUND INTERCEPT)
      READ(4,55) BCKR
55    FORMAT(F6.2)
      WRITE(4,56)
56    FORMAT(16H BACKGROUND SLOPE)
      READ(4,57) SLP
57    FORMAT(F6.3)
      M1=P1
      N1=S1
      M2=M1+N1*3
      DO 60 I=1,M2
      R=I
      P=(1./(S1*2.51))*(EXP(-0.5*((R-P1)/S1)**2))
     Y1=SLP*R+BCKR
      P=P*AREA1+Y1
      IX(I)=P
60    CONTINUE
      M2=M2+1
      DO 65 I=M2,NCHN
      R=I
      P=(1./(S2*2.51))*(EXP(-0.5*((R-P2)/S2)**2))
      Y2=SLP*R+BCKR
      P=P*AREA2+Y2
      IX(I)=P
65    CONTINUE
      WRITE(4,66)
66    FORMAT(6H TITLE)
      READ(4,67)(TITLE(I), I=1,15)
67    FORMAT(1A5,A2)
      WRITE(6,70)(TITLE(I), I=1,15)
70    FORMAT(1X,1A5,A2)
      WRITE(6,75)(IX(I), I=1,NCHN)
75    FORMAT(1X,I6)
      END
```

```
R

.DAT    DEVICE  USE

 -15     DTA0   OUTPUT
 -14     DTA1   INPUT
 -13     DTB1   OUTPUT FOR MACRO, F4
 -12     TTA0   LISTING
 -11     DTB1   INPUT FOR MACRO, F4
 -10     PRA0   INPUT
 -7      DTC0   SYS DEV FOR .SYSLD
 -6      DTB1   OUTPUT FOR CHAIN
 -5      NONE   USER LIBR FOR .LOAD
 -4      DTC1   SYS INPUT
 -3      TTA0   TTY OUT
 -2      TTA0   TTY IN
 -1      DTC0   SYS DEV FOR .LOAD
  1      DTA0   USER
  2      DTA1   USER
  3      DTA2   USER
  4      TTA0   USER
  5      PRA0   USER
  6      PPA0   USER
  7      XFA0   USER
  10     SCA0   USER

S
```